Development/Plasticity/Repair

The Neocortical Progenitor Specification Program Is Established through Combined Modulation of SHH and FGF Signaling

Odessa R. Yabut,[1] Hui-Xuan Ng,[1] Keejung Yoon,[1,2] Jessica C. Arela,[1] Thomas Ngo,[3] and Samuel J. Pleasure[1,4]
[1]Department of Neurology, University of California San Francisco, San Francisco, California 94158, [2]College of Biotechnology and Bioengineering, Sungkyunkwan University, Gyeonggi-do 440-746, Suwon, Republic of Korea, [3]Department of Psychiatry, University of California San Francisco, San Francisco, California 94143, and [4]Programs in Neuroscience and Developmental Biology, Eli and Edythe Broad Center of Regeneration Medicine and Stem Cell Research, University of California San Francisco, San Francisco, California 94143

Neuronal progenitors in the developing forebrain undergo dynamic competence states to ensure timely generation of specific excitatory and inhibitory neuronal subtypes from distinct neurogenic niches of the dorsal and ventral forebrain, respectively. Here we show evidence of progenitor plasticity when Sonic hedgehog (SHH) signaling is left unmodulated in the embryonic neocortex of the mammalian dorsal forebrain. We found that, at early stages of corticogenesis, loss of Suppressor of Fused (Sufu), a potent inhibitor of SHH signaling, in neocortical progenitors, altered the transcriptomic landscape of male mouse embryos. Ectopic activation of SHH signaling occurred, via degradation of Gli3R, resulting in significant upregulation of fibroblast growth factor 15 (*FGF15*) gene expression in all E12.5 Sufu-cKO neocortex regardless of sex. Consequently, activation of FGF signaling, and its downstream effector the MAPK signaling, facilitated expression of genes characteristic of ventral forebrain progenitors. Our studies identify the importance of modulating extrinsic niche signals such as SHH and FGF15, to maintain the competency and specification program of neocortical progenitors throughout corticogenesis.

Key words: **corticogenesis; FGF; lineage fates; neural progenitors; neurogenesis; SHH**

Significance Statement

Low levels of FGF15 control progenitor proliferation and differentiation during neocortical development, but little is known on how *FGF15* expression is maintained. Our studies identified SHH signaling as a critical activator of *FGF15* expression during corticogenesis. We found that Sufu, via Gli3R, ensured low levels of *FGF15* was expressed to prevent abnormal specification of neocortical progenitors. These studies advance our knowledge on the molecular mechanisms guiding the generation of specific neocortical neuronal lineages, their implications in neurodevelopmental diseases, and may guide future studies on how progenitor cells may be used for brain repair.

Introduction

The adult mammalian neocortex is composed of an intricate network of diverse excitatory and inhibitory neurons derived from distinct progenitor domains of the embryonic forebrain. Excitatory neurons originate from the ventricular zones (VZs) and subventricular zones (SVZs) of the embryonic neocortex, while inhibitory neurons (interneurons) originate from the ganglionic eminences (GEs). During corticogenesis, radial glial (RG) progenitors populating the VZ/SVZ sequentially generate deep-layer excitatory neurons, followed by upper-layer excitatory neurons via intermediate progenitor cell (IPC) or outer RG cells (Beattie and Hippenmeyer, 2017). This process must be tightly regulated since an imbalance between excitatory and inhibitory activity underlies a number of neurologic and neuropsychiatric disorders (Sohal and Rubenstein, 2019).

A combination of intrinsic and extrinsic cues guide and maintain the specification program of neocortical progenitors throughout corticogenesis to generate neuronal diversity. But the molecular factors integrating these cues in neocortical progenitors to produce distinct neuronal subtypes in a temporal manner are still largely unclear. Our previous work identified

Received Dec. 3, 2019; revised June 22, 2020; accepted July 18, 2020.

Author contributions: O.R.Y., H.-X.N., K.Y., and S.J.P. designed research; O.R.Y., H.-X.N., K.Y., J.C.A., and T.N. performed research; O.R.Y., H.-X.N., K.Y., J.C.A., T.N., and S.J.P. analyzed data; O.R.Y. and S.J.P. wrote the first draft of the paper; O.R.Y. and S.J.P. edited the paper; O.R.Y. and S.J.P. wrote the paper.

The authors declare no competing financial interests.

This work was supported by National Institutes of Health Grants R01s MH077694 and NS118995 to S.J.P., and National Institutes of Health/National Cancer Institute K01CA201068 and American Brain Tumor Association Grant #ARC1800003 to O.R.Y. and KNRF 2019M3A9H1103702 to K.Y. We thank members of the S. J.P. laboratory for helpful discussions; Dr. Kenneth Campbell for the Gsx2 antibody; and DeLaine Larsen and Kari Harrington (University of California San Francisco Nikon Imaging Center) for assistance with imaging.

Correspondence should be addressed to Samuel J. Pleasure at sam.pleasure@ucsf.edu.

https://doi.org/10.1523/JNEUROSCI.2888-19.2020

fundamental mechanisms at early stages of corticogenesis ensuring proper specification of neocortical progenitors into distinct excitatory neuronal lineages, through modulation of Sonic hedgehog (SHH) signaling pathway (Yabut et al., 2015). SHH signaling is triggered on binding of SHH ligands to the transmembrane receptor Patched 1 (Ptch1), which relieves its inhibition of another transmembrane protein, Smoothened (Smo). Consequently, Smo initiates a cascade of intracellular events promoting the nuclear translocation of Gli, a family transcription factor, to activate SHH target gene expression. However, intracellular checkpoints are present to modulate SHH signaling. In the developing neocortex, Suppressor of Fused (Sufu), a potent inhibitor of SHH signaling, is highly expressed in neocortical progenitors modulating SHH signals to ensure the production of molecularly distinct upper and deep layer excitatory neurons (Yabut et al., 2015). SUFU exerted this effect by ensuring the stable formation of Gli transcription factors, the downstream effectors of SHH signaling. Specifically, loss of SUFU resulted in the degradation of the repressor form of Gli3 (Gli3R), the predominant Gli protein in the developing neocortex (Palma and Ruiz i Altaba, 2004; Fotaki et al., 2006; H. Wang et al., 2011; Wilson et al., 2012), leading to the production of misspecified neocortical progenitors by mid-corticogenesis. However, little is known on the identity of downstream molecular targets of SHH signaling or Gli3 in neocortical progenitors, and how deregulation of these targets because of uncontrolled SHH signaling might affect neocortical progenitor fates.

Here we show that endogenous levels of SHH, in the absence of Sufu, can sufficiently increase SHH signal transduction in neocortical progenitors, resulting in drastic changes in the transcriptomic landscape of the VZ/SVZ at early stages of corticogenesis. In accordance to our previous findings, ventral forebrain progenitor gene transcripts are already ectopically expressed in neocortical progenitors of embryonic (E) 12.5 neocortex mice lacking Sufu. Additionally, we find that activation of fibroblast growth factor (FGF) signaling, via the upregulated gene expression of *FGF15*, leads to the misspecification of progenitors, particularly affecting the production of IPCs. These novel findings reveal how uncontrolled SHH signaling and its downstream gene targets can redefine progenitor competency in the embryonic neocortex. Further, this underscores the importance of intrinsic cellular responses, via modulatory proteins, such as Sufu, to temporally restrain extrinsic niche signals that can influence progenitor identity and fate.

Materials and Methods

Animals. Mice carrying the floxed Sufu allele ($Sufu^{fl}$) were kindly provided by Chi-Chung Hui (University of Toronto) and were genotyped as described previously (Pospisilik et al., 2010). *Emx1-cre* (stock #05628), *Rosa-AI14* (stock #007908), and *SmoM2* (stock #005130) mice were obtained from The Jackson Laboratory. Mice with the genotype *Emx1-cre*;$Sufu^{fl/fl}$ mice are hereto referred to as Sufu-cKO mice. Mice designated as controls did not carry the *Cre* transgene and may have either one of the following genotypes: $Sufu^{fl/+}$ or $Sufu^{fl/fl}$. All mouse lines were maintained in mixed strains, and analysis included male and female pups from each age group, although sex differences were not included in data reporting. All animal protocols were in accordance to the National Institute of Health regulations and approved by the University of California San Francisco Institutional Animal Care and Use Committee.

RNA-Seq and analysis. The dorsal forebrain was dissected from E12.5 control and Sufu-cKO male littermates ($n = 4$ per group). Total RNA was extracted using RNEasy Mini Kit (QIAGEN) and prepared for RNAseq. RNASeq was conducted by the University of California San Francisco Functional Genomics Core. Barcoded sequencing libraries were generated using the Truseq Stranded mRNA Library Prep Kit (Illumina). Single-end 50 bp reads were sequenced on the HiSeq4000 (Illumina). Sequencing yielded ~343 million read with an average read depth of 42.9 million reads/sample. Reads were then aligned using STAR_2.4.2a to the mouse genome (Ensembl Mouse GRCm38.78), and those that mapped uniquely to known mRNAs were used to assess differential expression (DE). Final quantification and statistical testing of differentially expressed (adjusted $p < 0.05$) genes were performed using DESeq2. Gene set enrichment and pathway analysis was conducted using the DAVID Gene Functional Classification Tool (http://david.abcc.ncifcrf.gov) (Huang et al., 2007). Heatmaps represent transformed FPKM values (Transform 1+ Log2(Y)) and plotted using Prism 8.1 (GraphPad). Filtering was applied for gene ontology enrichment analysis by excluding DE genes with very low normalized read counts (FPKM <100) in both control and mutant samples. Sequencing data are archived in the Gene Expression Omnibus under GEO Accession # GSE155851.

Immunohistochemistry. Perfusion, dissection, and immunofluorescence staining were conducted according to standard protocols as previously described (Siegenthaler et al., 2009). Briefly, embryonic brain tissues were fixed by direct immersion in 4% PFA and postnatal brains fixed by intracardial perfusion followed by 2 h after fixation. Cryostat sections were air-dried and rinsed 3× in PBS plus 0.2% Triton before blocking for 1 h in 10% normal lamb serum diluted in PBS with 0.2% Triton to prevent nonspecific binding. A heat-induced antigen retrieval protocol was performed on selective immunohistochemistry using 10 μM citric acid at pH 6.0. Primary antibodies were diluted in 10% serum diluted in PBS with 0.2% Triton containing DAPI; sections were incubated in primary antibody overnight at room temperature. The following antibodies were used: rabbit anti-Tbr2 (1:500 dilution; Abcam, #ab23345), rabbit anti-GSX2 (1:250 dilution; gift from Kenneth Campbell) (Toresson et al., 2000), mouse anti-Olig2 (1:250 dilution; Millipore, #MABN50), and phosphorylated-Erk1/2 (pERK1/2 1:100 dilution, Cell Signaling Technology, #4370). To detect primary antibodies, we used species-specific AlexaFluor-conjugated secondary antibodies (1:500; Invitrogen) in 1× PBS-T for 1 h at room temperature, washed with 1× PBS, and coverslipped with Fluoromount-G (Southern Biotechnology).

ISH. Lhx2, CoupTF2 ISH was conducted using RNA probes kindly provided by Professor John Rubenstein (University of California San Francisco). Dlx1 and Dbx1 riboprobes were generated using primer sequences published by the Allen Brain Atlas *ISH* Database (http://developingmouse.brain-map.org/) with SP6 and T7 promoter binding sequences included in 5′ ends. Target gene cDNA was amplified from pooled cDNA reactions made from mouse brain; total RNA was used as a template source. DIG-labeled RNA probes were generated using the DIG RNA Labeling Kit SP6/T7 (Sigma Millipore, catalog #11175025910) according to the manufacturer's protocols. DIG-labeled RNA probes were diluted in hybridization buffer (50% formamide, 5 × SSC, 0.3 mg/ml tRNA, 100 µl/ml heparin, 1× Denhardt's solution, 0.1% Tween 20, 0.1% CHAPS, 5 mM EDTA) and added to RNase-free cryosections for incubation in a humidified chamber at 65°C for 16-20 h. Sections were washed in 0.2 × SSC (Ambion, AM9770) at 65°C followed by PBST at room temperature. Tissue sections were incubated in alkaline phosphatase-conjugated anti-DIG antibody (1:1500, Roche Applied Sciences, 11093274910) for 16-20 h incubation at room temperature, and colorimetric signals were detected using NBT/BCIP (Roche Applied Sciences, 11383221001).

RNAScope ISH was conducted for *Fgf15* and *PTCH1*. RNAscope probes Mm-Ptch1 (catalog #402811) and Mm-FGF15 (catalog #412811) were designed commercially by the manufacturer (Advanced Cell Diagnostics). RNAScope Assay was performed using the RNAscope Multiplex Fluorescent Reagent Kit V2 according to the manufacturer's instructions. Detection of the probe was done with Opal 570 or Opal 520 reagent (PerkinElmer).

Forebrain organotypic slice culture. Whole brains from E12.5 WT CD-1 mice were carefully dissected and placed in ice-cold HBSS (Invitrogen). Brains were embedded in 4% Low Melting Point Agarose (Nueve)/HBSS mix and allowed to solidify on ice. Embedded brains were sliced using a VT1000S vibratome (Leica Microsystems) into 400-µm-thick slices and placed in Recovery Media: MEM (Invitrogen) with Glutamax (Invitrogen) and pennicillin/streptomycin (Invitrogen). Slices

Table 1. Statistical analyses[a]

Figure	Parameter	Groups	Statistical test	Outcome	*p*
5D	E12.5 phospho-Erk1/2$^+$ regions	A-P position vs genotype (E12.5 control and Sufu-cKO)	Repeated-measures two-way ANOVA	F position × genotype (3,24) = 3.329	0.0365
		Control (n = 5) vs Sufu-cKO (n = 5) Position 1	Holm-Sidak's multiple comparisons test	t = 3.685, df = 5.547	0.018
		Control (n = 5) vs Sufu-cKO (n = 5) Position 2		t = 6.861, df = 4.873	0.0033
		Control (n = 5) vs Sufu-cKO (n = 5) Position 3		t =8.112, df = 4.949	0.0019
		Control (n = 5) vs Sufu-cKO (n = 5) Position 4		t = 5.310, df = 4.296	0.0099
5E	E14.5 phospho-Erk1/2$^+$ regions	A-P position vs genotype (E14.5 control and Sufu-cKO)	Repeated-measures two-way ANOVA	F position vs genotype (3,19) = 4.684	0.013
		Control (n = 4) vs Sufu-cKO (n = 3) Position 1	Holm-Sidak's multiple comparisons test	t = 7.255, df = 27	<0.0001
		Control (n = 5) vs Sufu-cKO (n = 5) Position 2		t = 5.452, df = 27	<0.0001
		Control (n = 5) vs Sufu-cKO (n = 5) Position 3		t = 4.665, df = 27	0.0001
		Control (n = 4) vs Sufu-cKO (n = 4) Position 4		t = 3.67, df = 27	0.0011
6D	Tbr2$^+$ cells	Treatment (n = 3 per condition)	One-way ANOVA	F treatment (5,12) = 14.15	0.0001
		DMSO vs Fgf15	Holm-Sidak's multiple comparisons test	t = 3.319, df = 12	0.0537
		DMSO vs Shh		t = 6.515, df = 12	0.0004
		DMSO vs Fgf15+Shh		t = 5.651, df = 12	0.0014
		DMSO vs Cyclo		t = 0.5662, df = 12	0.6585
		DMSO vs Cyclo+Fgf15		t = 4.4, df = 12	0.0095
		Fgf15 vs Shh		t = 3.196, df = 12	0.0599
		Fgf15 vs Fgf15+Shh		t = 2.332, df = 12	0.2072
		Fgf15 vs Cyclo		t = 2.753, df = 12	0.1163
		Fgf15 vs Cyclo+Fgf15		t = 1.081, df = 12	0.6585
		Shh vs Fgf15+Shh		t = 0.8646, df = 12	0.6585
		Shh vs Cyclo		t = 5.949, df = 12	0.0009
		Shh vs Cyclo+Fgf15		t = 2.115, df = 12	0.2503
		Fgf15+Shh vs Cyclo		t = 5.085, df = 12	0.0032
		Fgf15+Shh vs Cyclo+Fgf15		t = 1.251, df = 12	0.6572
		Cyclo vs Cyclo+Fgf15		t = 3.834, df = 12	0.0235
7I	Tbr2$^+$ cells	Treatment: DMSO (n = 6) vs FGF15 (n = 6)	Unpaired t test (two-tailed)	t = 2.805, df = 10	0.0186

[a]Summary of statistical analyses performed for Figures 5-7.

were transferred into uncoated Millicell-CM membrane inserts (EMD Millipore) in 6-well plates (BD Biosciences) and cultured in Neurobasal (Invitrogen) supplemented with Glutamax (Invitrogen), pennicillin/streptomycin (Invitrogen), B-27 (Invitrogen), and N2 (Invitrogen) at 37°C, 5% CO_2, and 100% humidity. After 2 DIV, cell culture media were aspirated, and slices were washed in 1× PBS, fixed in cold 4% PFA for 30 min, cryoprotected in 30% sucrose, and embedded in OCT. Slices were cryosectioned into 20-µm-thick coronal sections and stored at −80°C until used for immunofluorescence analysis as described above. Treatment (as described in text) of organotypic slices was conducted 2-3 h after initial plating and incubation of slices with the following concentrations: 100 ng/ml recombinant FGF15 (Prospec Bio, #CYT-027), 200 ng/ml recombinant SHH (GenScript, #Z03050-50), and 5 µM cyclopamine (Toronto Research Chemicals, #C988400). Following treatments, slice cultures were incubated for 2 d and processed as described above.

Image analysis and acquisition. Images were acquired using a Nikon EDC microscope equipped with a QCapture Pro camera (QImaging), Axioscan Z.1 (Carl Zeiss) using the Zen 2 blue edition software (Carl Zeiss), or the Nikon Ti inverted microscope with CSU-W1 large FOV confocal and Andor Zyla 4.2 sCMOS camera. All images were imported in tiff or jpeg format. Brightness, contrast, and background were adjusted equally for the entire image between controls and mutant using the "Brightness/Contrast" and "Levels" function from "Image/Adjustment" options in Adobe Photoshop or National Institutes of Health ImageJ without any further modification. National Institutes of Health ImageJ was used to threshold background levels between controls and mutant tissues to quantify fluorescence labeling. For pErk1/2 quantification, the total area with positive pErk1/2 labeling was measured, which began in the pallial-subpallial boundary in the controls and extended dorsally in Sufu-cKO neocortex, for each hemisphere across the anterior to posterior axis. One forebrain section in each representative anterior to posterior region was measured (see Fig. 5C) from both hemispheres and averaged. All analyses were conducted in at least two or three 20-µm-thick sections that were histologically matched at the rostral-caudal level between genotypes.

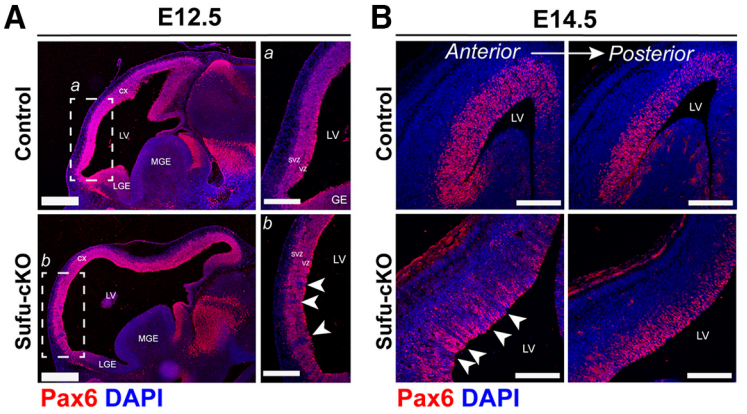

Figure 1. Neocortical progenitor defects are evident in discrete regions in the E12.5 Sufu-cKO neocortex. ***A***, Immunofluorescence staining of sagittal sections of E12.5 control and Sufu-cKO embryonic forebrains, using dorsal forebrain progenitor marker, Pax6, and DAPI counterstain, shows high Pax6 expression in the dorsal forebrain (CX) along the lateral ventricles (LV) compared with the lateral (LGE) or medial (MGE) GE in both genotypes. ***A***, ***B***, Higher magnification of boxed regions represents low or absent Pax6 expression in specific areas of the anterior neocortex of Sufu-cKO forebrains (arrows, *b*) particularly in the VZ and SVZ but not in controls (*a*). These defects were not evident in the E10.5 Sufu-cKO or control forebrains (Extended Data Fig. 1-1). Sections are counterstained with DAPI. Scale bars: ***A***, ***B*** 500 µm; *a*, *b*, 250 µm. ***B***, Pax6 immunofluorescence staining of coronal sections of the E14.5 control and Sufu-cKO represents areas lacking Pax6 expression in the anterior neocortex of the E14.5 Sufu-cKO mice (arrows) but not in posterior regions or in controls. Scale bar, 200 µm.

Statistics. Prism 8.1 (GraphPad) was used for statistical analysis. Two-sample experiments were analyzed by Student's t test, and experiments with more than two parameters were analyzed by ANOVA. In

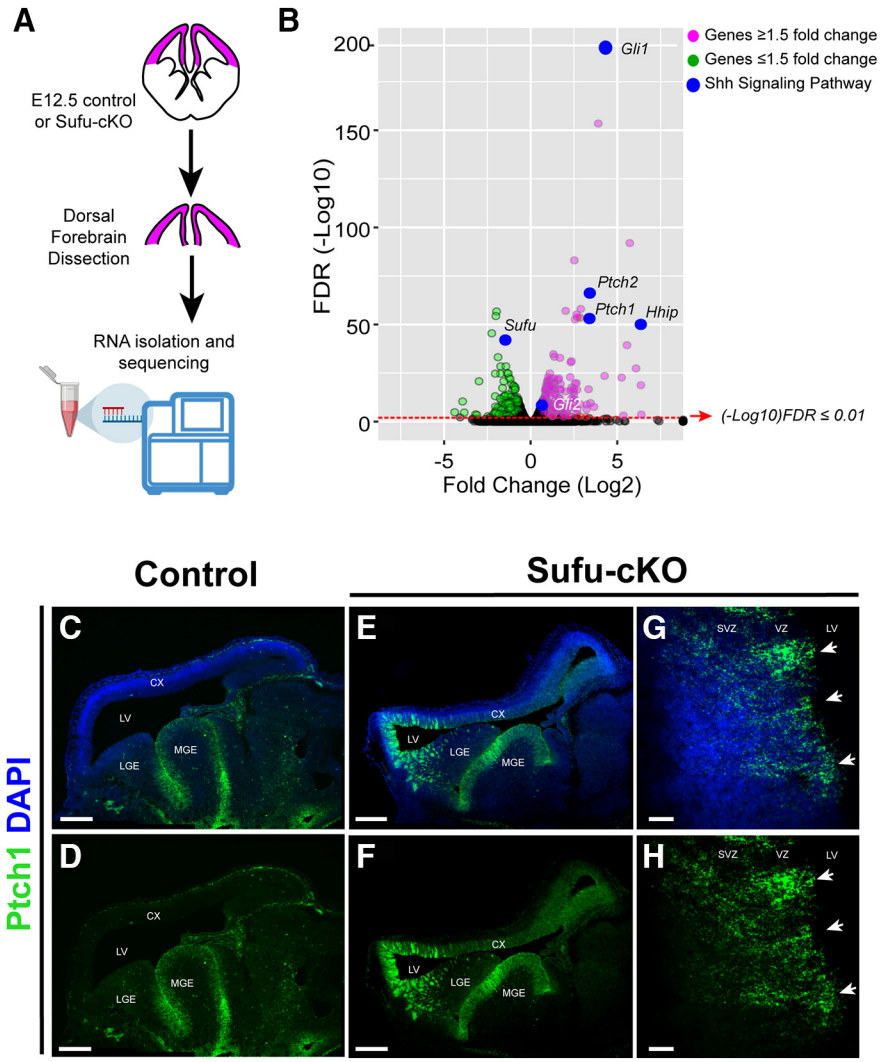

Figure 2. Upregulated expression of SHH signaling gene targets in neocortical progenitors of the E12.5 Sufu-cKO dorsal forebrain. ***A***, Schematic showing dorsal forebrain areas (pink) dissected from control and mutant E12.5 mice for RNA-Seq analysis. ***B***, Volcano plot of RNA-Seq dataset highlighting differentially expressed genes with adjusted p value < 0.01 (FDR (-Log10)) and fold change (Log2) ≥ 1.5 (red circles) or fold change (Log2) ≤ 1.5 (green circles), and genes in the SHH signaling pathway (blue circles), between the E12.5 dorsal forebrain of controls and Sufu-cKO E12.5 embryos (see also Tables 2 and 3). ***C–F***, RNAscope ISH on sagittal brain sections using probes for Patched 1 (Ptch1) validates upregulation of Ptch1 RNA expression in the E12.5 Sufu-cKO dorsal forebrain (***E***,***F***), whereas Ptch1 RNA expression is only detected in the MGE of controls (***C***,***D***). ***C***, ***E***, Sections are counterstained with DAPI. Scale bar, 500 µm. ***G***, ***H***, Higher magnification of rostral neocortex of E12.5 Sufu-cKO dorsal forebrain showing that Ptch1 RNA expression is preferentially higher along the VZ and SVZ where neocortical progenitors are localized. Ptch1 expression also appear in columns, radiating inward from the apical VZ (arrows). ***G***, Sections are counterstained with DAPI. Scale bar, 25 µm.

one- or two-way ANOVA, when interactions were found, follow-up analyses were conducted for the relevant variables using Holm-Sidak's multiple comparisons test. All experiments were conducted at least in triplicate with sample sizes of $n = 3$-6 embryos/animals/slices per genotype. A p value ≤ 0.05 was considered statistically significant. Graphs represent mean ± SEM. Statistical values and analyses are summarized in Table 1.

Results

Specification defects are evident in discrete regions of the neocortex of E12.5 embryonic mice lacking Sufu

The role of SHH signaling in neocortical neuron specification is critical before E13.5, a time point at which superficial projection neurons are just beginning to differentiate. Analysis of mice, in which Sufu is conditionally deleted at E10.5 in neocortical progenitors using the Emx1-Cre driver (*Emx1-cre/+;Sufu-fl/fl* or Sufu-cKO), revealed that modulating SHH signaling is critical to properly specify distinct superficial and deep layer projection neurons, after dorsoventral patterning of the forebrain (Yabut et al., 2015). While specification defects were clear at E14.5 in Sufu-cKO cortex, any molecular changes before this time point were not deeply examined in the previous study. Since changes in Gli2 and Gli3R levels were apparent at E12.5, we postulated that critical molecular alterations must have occurred at this time point. We therefore initiated our studies by careful examination of Pax6 expression, which is highly expressed in neocortical RG progenitors (Ypsilanti and Rubenstein, 2016). As expected, we found that Pax6 exclusively expressed in dorsal forebrain regions of the E12.5 control and Sufu-cKO brains, and not in the GE (Fig. 1*A*). However, Pax6 expression was noticeably intermittent in anterior regions of the E12.5 Sufu-cKO neocortex (Fig. 1*Ab*, boxed regions, arrowheads). Moreover, these Pax6-negative areas exhibited a columnar distribution hinting at anomalous RG clones. Analysis of corresponding regions showed that the E14.5 Sufu-cKO neocortex similarly displayed columnar distribution of $Pax6^+$ and $Pax6^-$ regions in anterior regions (Fig. 1*B*, arrowheads), but this distribution was not prevalent in posterior regions (Fig. 1*B*). These defects were not present at E10.5, in which the distribution of $Pax6^+$ cells were largely indistinguishable between controls and Sufu-cKO embryos (Extended Data Fig. 1-1). Therefore, despite having properly formed dorsal forebrain domains, a subpopulation of neocortical RG progenitors displayed aberrant behavior in the E12.5 Sufu-cKO neocortex.

Upregulated expression of SHH signaling targets in Sufu mutant neocortical progenitors

To better understand the molecular changes in neocortical progenitors of the E12.5 Sufu-cKO neocortex, we isolated total RNA from dissected control and mutant dorsal forebrain for transcriptome profiling by RNA-Seq (Fig. 2*A*). Sequencing yielded ~343 million reads with an average read depth of 42.9 million reads/sample ($n = 4$ per genotype). Reads were then aligned to the mouse genome, and we successfully mapped 98.69 ± 0.04% of the fragments to the genome, with 17.01 ± 0.11% of fragments mapped to multiple locations of the genome. Those that mapped uniquely to known mRNAs (81.68 ± 0.12% of fragments) were used to assess DE. Differentially expressed genes (with average FPKM > 20 in at least one sample/genotype group) were assessed (Table 2).

We confirmed that SHH signaling gene targets, such as *Gli1*, *Patched 1* and *2* (*Ptch1* and *Ptch2*), and the *Hedgehog-Interacting*

Table 2. Top differentially expressed genes between E12.5 control and Sufu-cKO dorsal forebrain[a]

		Mutant vs control				Controls (FPKM)		Sufu-cKO (FPKM)	
Ensembl_ID	Gene	FC	Log2 FC	RawP	FDR	Average	SD	Average	SD
ENSMUSG00000075707	Dio3	82.3875172	6.36435386	4.7499E-22	1.7416E-19	7.96831358	4.59579515	656.489572	229.835653
ENSMUSG00000064325	Hhip	82.0823811	6.35900068	6.0704E-54	9.0338E-51	8.91857894	2.87906586	732.058195	155.710915
ENSMUSG00000097758	Dio3os	69.4175062	6.11722763	1.4018E-41	1.612E-38	5.84745817	5.83167716	405.915963	93.8868307
ENSMUSG00000032517	Mobp	67.8055024	6.08333045	5.5873E-31	4.2835E-28	1.86323925	2.34119106	126.337874	31.3170661
ENSMUSG00000031073	Fgf15	52.7038764	5.71983717	1.3756E-96	1.16E-92	152.277335	111.900656	8025.60586	1237.95433
ENSMUSG00000045608	Dbx2	47.1893736	5.56039012	3.7256E-43	4.4882E-40	3.38315277	2.99144763	159.64886	31.6909208
ENSMUSG00000049796	Crh	40.8306688	5.35158129	2.1529E-05	0.00081173	3.26686208	3.21281656	133.388164	93.6383147
ENSMUSG00000030507	Dbx1	38.0194446	5.24866555	3.6317E-26	2.0881E-23	27.7421756	13.2249167	1054.74211	301.451019
ENSMUSG00000040543	Pitpnm3	19.2787426	4.26893905	4.7584E-27	3.0096E-24	10.5181239	1.3609172	202.776203	48.0779528
ENSMUSG00000025407	Gli1	18.6364862	4.22005797	3.99E-198	1.009E-193	81.5909417	30.4343144	1520.56846	123.97597
ENSMUSG00000038156	Spon1	14.9532123	3.90238353	2.55E-158	3.225E-154	56.2092056	22.9496826	840.508183	67.3977619
ENSMUSG00000096999	Gm26793	13.902041	3.7972248	1.3196E-66	4.7694E-63	15.772933	4.61397622	219.275962	28.1418305
ENSMUSG00000039830	Olig2	12.6102384	3.65652365	2.65E-10	2.7033E-08	69.5186604	19.2058548	876.646882	335.706
ENSMUSG00000022705	Drd3	10.9351284	3.45089825	1.7866E-12	2.5537E-10	2.96186159	2.09340292	32.3883366	5.63433683
ENSMUSG00000028681	Ptch2	10.6406223	3.41151062	1.5859E-70	6.687E-67	52.6270255	16.7143266	559.984299	68.0032837
ENSMUSG00000021466	Ptch1	10.5027097	3.39268968	5.0105E-57	8.4508E-54	692.640882	117.331353	7274.60609	1053.60989
ENSMUSG00000044220	Nkx2-3	10.1453116	3.34274127	7.382E-20	2.1222E-17	34.6890788	7.47294372	351.931514	86.7310817
ENSMUSG00000063600	Egfem1	9.46791651	3.24304698	1.358E-11	1.6759E-09	10.8922792	6.68726483	103.12719	32.3185231
ENSMUSG00000046160	Olig1	9.35940117	3.22641623	4.6615E-09	3.905E-07	6.21737577	1.93182166	58.1909141	21.2357905
ENSMUSG00000035946	Gsx2	9.19782474	3.20129271	8.7129E-05	0.00271461	40.8981257	51.8805517	376.173792	198.118943
ENSMUSG00000085072	Ict1os	7.94959453	2.99088128	2.0916E-13	3.4361E-11	5.31695799	2.76251218	42.2676602	8.90946841
ENSMUSG00000028370	Pappa	7.41766068	2.89096427	2.9723E-62	9.3997E-59	293.550189	58.6301674	2177.45569	265.650782
ENSMUSG00000102796	RP23-335B9.5	7.31629286	2.87111282	4.655E-11	5.353E-09	4.77449345	4.42629104	34.9315923	3.48684994
ENSMUSG00000030862	Cpxm2	7.24779323	2.8575418	1.7851E-57	3.2258E-54	39.618948	11.0091521	287.149943	5.16012755
ENSMUSG00000045591	Olig3	7.20471446	2.84894125	8.3417E-12	1.0658E-09	5.25145549	3.63879005	37.8352373	3.88669789
ENSMUSG00000003227	Edar	7.07128346	2.82197209	4.5951E-05	0.00156886	14.2573202	6.28628971	100.817552	49.3383641
ENSMUSG00000036466	Megf11	6.46970608	2.69370017	5.4537E-09	4.4364E-07	65.0626058	12.0041891	420.935937	144.39887
ENSMUSG00000074785	Plxnc1	6.4646009	2.69256131	1.0379E-57	2.0198E-54	1220.54603	85.3997809	7890.34299	984.760757
ENSMUSG00000099907	Gm10421	6.39502413	2.6769498	0.00019259	0.00527872	5.31695799	2.76251218	34.0020746	17.1217016
ENSMUSG00000031075	Ano1	6.35732479	2.6684198	1.743E-19	4.7931E-17	195.346022	110.705417	1241.87811	247.642224
ENSMUSG00000022123	Scel	6.32244811	2.66048329	2.1846E-06	0.00010235	3.17234829	1.39922353	20.0570074	4.89357975
ENSMUSG00000092035	Peg10	6.27994507	2.65075194	2.8891E-59	6.6448E-56	3817.18429	700.861794	23971.7077	2841.06804
ENSMUSG00000050447	Lypd6	6.23322426	2.63997862	3.7257E-23	1.5452E-20	714.738273	124.510077	4455.12394	879.153524
ENSMUSG00000086296	D030055H07Rik	6.19868743	2.63196276	5.2197E-08	3.5594E-06	237.148775	233.241004	1470.01113	483.09669
ENSMUSG00000030554	Synm	5.94385294	2.57139842	1.6757E-56	2.6495E-53	175.969431	16.7160858	1045.93642	126.207302
ENSMUSG00000079502	1700101E01Rik	5.92186351	2.56605124	4.8084E-23	1.9621E-20	21.9274193	4.44864992	129.851184	24.1986298
ENSMUSG00000026344	Lypd1	5.78045668	2.53118348	1.6816E-14	3.0827E-12	108.297771	11.4653093	626.010575	155.439255
ENSMUSG00000052301	Doc2a	5.74190592	2.52152969	1.507E-87	9.5315E-84	147.465778	24.7584518	846.734623	64.6720575
ENSMUSG00000036264	Fstl4	5.66355645	2.50170828	8.1061E-10	7.4573E-08	7.06205978	5.2274176	39.9963742	10.1087574
ENSMUSG00000027832	Ptx3	5.62037022	2.49066516	3.7632E-20	1.1334E-17	323.719795	71.905768	1819.4251	368.556876
ENSMUSG00000025856	Pdgfa	5.60936415	2.48783724	8.4139E-17	1.9529E-14	213.357738	41.0886507	1196.80125	267.580448
ENSMUSG00000039579	Grin3a	5.57374247	2.47864634	1.1749E-12	1.7382E-10	23.3137923	14.1868649	129.945074	30.2336844
ENSMUSG00000020902	Ntn1	5.5507006	2.47266988	1.2616E-18	3.1918E-16	182.967354	114.72434	1015.597	180.417925
ENSMUSG00000015501	Hivep2	5.36960862	2.42481694	2.9316E-27	1.9017E-24	366.270823	58.4251106	1966.73097	333.806373
ENSMUSG00000026765	Lypd6b	5.15521956	2.36603387	7.9847E-21	2.658E-18	64.128181	21.8461262	330.594853	59.9726836
ENSMUSG00000071862	Lrrtm2	5.15367748	2.36560226	5.4108E-15	1.0573E-12	99.5065322	21.4481348	512.824574	118.534936
ENSMUSG00000044499	Hs3st5	5.1458571	2.36341139	0.00036629	0.00909391	5.29148754	6.35506294	27.2292387	11.371032
ENSMUSG00000022449	Adamts20	5.09486349	2.34904349	8.4761E-35	7.6584E-32	879.123707	153.586556	4479.01527	645.467259
ENSMUSG00000047935	Gm5607	5.07145449	2.34239957	1.5793E-17	3.8051E-15	235.233075	84.7104464	1192.97383	238.817078
ENSMUSG00000050511	Oprd1	5.01904508	2.32741291	3.4705E-19	9.0517E-17	18.3322572	2.46129774	92.0104253	8.50394075
ENSMUSG00000042942	Greb1l	4.97801523	2.31557065	3.1282E-34	2.729E-31	40.9347158	11.732061	203.773639	24.7529018
ENSMUSG00000024565	Sall3	4.87269605	2.28472023	1.9085E-26	1.1496E-23	323.047376	135.817299	1574.11167	225.027015
ENSMUSG00000050830	Vwc2	4.77175349	2.25451952	4.5876E-10	4.4985E-08	15.1718669	6.17372207	72.3964088	19.3261315
ENSMUSG00000079042	Trim61	4.65688672	2.21936579	2.3428E-05	0.00087679	13.1499629	7.22679895	61.2378877	23.6763672
ENSMUSG00000020182	Ddc	4.23590166	2.0826691	9.4268E-08	5.9622E-06	20.3591524	11.1225092	86.2393673	24.3118885
ENSMUSG00000047773	Ankfn1	4.21116097	2.07421802	1.1688E-07	7.1944E-06	24.0803028	16.5671624	101.406031	27.6755788
ENSMUSG00000024302	Dtna	4.18161594	2.06406056	5.1632E-12	6.8081E-10	338.390772	40.517148	1415.02025	341.918631
ENSMUSG00000036800	Fam135b	4.12972627	2.04604616	6.3431E-08	4.1682E-06	9.42253743	4.08437337	38.9125003	3.17059338
ENSMUSG00000074607	Tox2	4.05513698	2.01975065	3.3761E-61	9.4903E-58	214.277748	34.3114331	868.925619	45.6255507
ENSMUSG00000075585	6330403L08Rik	4.04965382	2.01779859	1.1438E-23	4.9045E-21	81.839912	11.821983	331.423312	52.4601701
ENSMUSG00000079022	Col22a1	3.99687359	1.99887194	1.1506E-18	2.9403E-16	190.333392	55.8880568	760.738507	130.864341
ENSMUSG00000042596	Tfap2d	3.97894006	1.99238417	3.5297E-05	0.00124026	5.85024556	2.80274705	23.2777764	4.85423132
ENSMUSG00000051111	Sv2c	3.85688177	1.94743492	3.5418E-10	3.5557E-08	14.2768431	2.80800532	55.0640958	13.2925298

(*Table continues*.)

Table 2. Continued

		Mutant vs control				Controls (FPKM)		Sufu-cKO (FPKM)	
Ensembl_ID	Gene	FC	Log2 FC	RawP	FDR	Average	SD	Average	SD
ENSMUSG00000068615	Gjd2	3.80184566	1.92669997	1.1779E-06	5.9128E-05	61.7032342	36.9856894	234.586174	66.2654422
ENSMUSG00000098720	Gm27239	3.77853425	1.9178267	8.3282E-06	0.00034082	11.659048	6.54292995	44.0541121	13.7787559
ENSMUSG00000049001	Ndnf	3.73392102	1.90069141	8.9513E-05	0.00277523	84.3597985	25.815264	314.992825	125.895367
ENSMUSG00000086166	Gm14342	3.73258508	1.90017514	0.00010402	0.00312902	27.0665733	5.77653922	101.028288	41.3763515
ENSMUSG00000089706	B230216N24Rik	3.72899772	1.89878791	5.5728E-09	4.5044E-07	23.7767168	2.64105515	88.6633225	23.6271382
ENSMUSG00000074664	A830092H15Rik	3.62105772	1.85641117	1.7952E-08	1.3203E-06	13.2193334	4.881595	47.8679692	8.86801891
ENSMUSG00000104362	RP23-14P23.9	3.61176286	1.85270317	2.0555E-05	0.00077731	10.3499453	4.08943513	37.381548	12.6185099
ENSMUSG00000020123	Avpr1a	3.53639057	1.82227762	2.9151E-05	0.00105961	7.54764523	2.02605087	26.6914214	8.0009556
ENSMUSG00000047490	4932411E22Rik	3.36693844	1.75143734	0.0010747	0.02232278	27.1248819	21.6975709	91.3278074	37.0073908
ENSMUSG00000027359	Slc27a2	3.34193228	1.7406825	2.3462E-07	1.3708E-05	51.0149118	24.0038259	170.488381	42.7610472
ENSMUSG00000084530	Mir1897	3.33807121	1.73901473	1.2453E-16	2.8382E-14	62.1838633	9.85874007	207.574164	35.9326096
ENSMUSG00000029819	Npy	3.31923275	1.7308498	4.1568E-05	0.00143077	15.0866798	6.98499659	50.0762016	15.7778788
ENSMUSG00000025592	Dach2	3.31374172	1.72846116	1.4124E-19	3.9266E-17	158.016602	8.62214082	523.626206	86.5639353
ENSMUSG00000035547	Capn5	3.31187319	1.72764743	2.3752E-06	0.00011006	306.765239	58.2130529	1015.96757	314.538138
ENSMUSG00000032500	Dclk3	3.30608859	1.72512538	0.00064073	0.01455132	6.13236946	4.597098	20.2741567	6.1767319
ENSMUSG00000024247	Pkdcc	3.30382084	1.72413545	1.126E-22	4.1892E-20	1252.30821	125.627043	4137.40196	623.825098
ENSMUSG00000022860	Chodl	3.30288747	1.72372782	4.0662E-07	2.2559E-05	147.882007	7.0214577	488.437628	143.929506
ENSMUSG00000021136	Smoc1	3.28121386	1.71422963	5.2404E-06	0.00022471	195.520108	59.5128888	641.543288	199.481655
ENSMUSG00000026830	Ermn	3.23714959	1.69472404	5.2745E-20	1.5699E-17	54.9546928	8.40074396	177.896562	16.5042846
ENSMUSG00000044646	Zbtb7c	3.23051993	1.69176638	2.302E-05	0.00086408	37.9170557	7.37660091	122.491804	42.2116689
ENSMUSG00000033578	Tmem35	3.2302653	1.69165266	1.5958E-36	1.4952E-33	1127.90224	120.959094	3643.42348	409.033682
ENSMUSG00000040490	Lrfn2	3.18401969	1.67084926	7.2752E-15	1.3944E-12	39.1071952	12.2460043	124.518079	18.6795639
ENSMUSG00000054667	Irs4	3.13177691	1.64698145	2.9078E-13	4.6854E-11	49.9437875	19.1290241	156.4128	24.0937045
ENSMUSG00000040138	Ndp	3.12319172	1.64302113	2.4726E-12	3.4752E-10	95.7876009	34.8465532	299.163042	49.7002428
ENSMUSG00000050840	Cdh20	3.08850363	1.62690802	1.1083E-25	5.8416E-23	106.913709	10.6422135	330.203377	43.9172105
ENSMUSG00000041741	Pde3a	3.04396437	1.60595147	1.96E-15	3.9354E-13	187.16056	6.74657395	569.710077	101.903411
ENSMUSG00000040274	Cdk6	3.00977691	1.58965656	3.4118E-07	1.9266E-05	268.749406	56.463021	808.875758	221.889593
ENSMUSG00000000394	Gcg	2.9987494	1.58436096	5.1988E-05	0.00174898	10.1749288	2.41034037	30.5120615	0.85945099
ENSMUSG00000019996	Map7	2.98414601	1.57731813	6.4478E-25	3.0778E-22	209.157269	51.450683	624.15583	66.9975195
ENSMUSG00000098795	Gm27403	2.97740163	1.57405384	7.5553E-05	0.00239226	9.91687056	1.18391156	29.5265066	7.14880484
ENSMUSG00000040856	Dlk1	2.94421152	1.55788132	4.357E-11	5.0797E-09	263.480148	38.0180169	775.741286	160.128256
ENSMUSG00000028327	Stra6l	2.88800126	1.53007137	5.8469E-06	0.00024819	15.4399989	9.43780409	44.5907361	8.76982563
ENSMUSG00000097391	Mirg	2.87721896	1.52467502	1.5303E-24	7.1693E-22	167.971733	41.2167474	483.291455	49.2273237
ENSMUSG00000026834	Acvr1c	0.35355123	−1.5000088	4.2937E-05	0.00147191	93.2425331	29.3210588	32.9660125	8.18849727
ENSMUSG00000010136	Pifo	0.35177415	−1.5072786	8.6817E-09	6.7167E-07	105.332893	17.5768786	37.0533893	17.2886542
ENSMUSG00000070469	Adamtsl3	0.35144023	−1.5086487	9.3984E-05	0.00287509	116.613241	37.4732435	40.9825842	15.0234823
ENSMUSG00000051295	9630028B13Rik	0.35118393	−1.5097013	4.0463E-13	6.3189E-11	643.36647	113.057645	225.939965	42.8499072
ENSMUSG00000028332	Hemgn	0.35116061	−1.5097971	1.9812E-05	0.00075373	37.0090921	7.46377266	12.9961354	5.29317298
ENSMUSG00000026894	Morn5	0.35106389	−1.5101945	0.00013151	0.0037938	29.4578997	1.90296451	10.3416047	5.65284779
ENSMUSG00000066720	Cldn9	0.3501717	−1.5138656	3.0908E-16	6.859E-14	162.137617	9.81486786	56.7760045	13.3936847
ENSMUSG00000068323	Slc4a5	0.34982911	−1.5152778	4.9013E-06	0.0002116	257.959456	63.4364916	90.2417258	44.5794649
ENSMUSG00000061702	Tmem91	0.34906622	−1.5184273	0.00019235	0.00527792	28.2810443	4.41105244	9.87195722	3.35910125
ENSMUSG00000064280	Ccdc146	0.34880428	−1.5195104	5.4773E-06	0.00023368	67.6679945	14.7495157	23.6028859	13.8770235
ENSMUSG00000052221	Ppp1r36	0.34759815	−1.5245077	9.7323E-05	0.00296289	30.9282928	7.99832995	10.7506174	4.11878765
ENSMUSG00000026614	Slc30a10	0.34661665	−1.5285872	6.1789E-14	1.0932E-11	2625.06768	451.787567	909.892154	182.852362
ENSMUSG00000018776	Slc35g3	0.34231249	−1.5466142	3.0021E-05	0.00108499	33.0592156	4.42957456	11.3165824	5.39664868
ENSMUSG00000038194	Lhb	0.34189609	−1.5483702	8.3389E-06	0.00034082	50.9958392	11.7095001	17.4352781	10.4529431
ENSMUSG00000026494	Kif26b	0.34152931	−1.5499187	6.9904E-16	1.4737E-13	1646.16747	225.295325	562.214447	166.65265
ENSMUSG00000090122	Kcne1l	0.34137833	−1.5505566	3.8971E-24	1.7297E-21	303.070236	33.6744393	103.461611	16.3432342
ENSMUSG00000030650	Tmc5	0.34032659	−1.5550082	1.0979E-10	1.187E-08	85.4614915	9.13797157	29.0848177	5.99513518
ENSMUSG00000022636	Alcam	0.33836637	−1.5633419	7.7325E-11	8.58E-09	4518.20486	531.333737	1528.80859	785.618951
ENSMUSG00000028801	Stpg1	0.33680821	−1.5700008	0.00019721	0.00539364	28.022659	9.89051345	9.43826152	3.43802694
ENSMUSG00000030708	Dnajb13	0.33460891	−1.5794522	1.0653E-11	1.3476E-09	97.9384992	10.9025795	32.7710949	13.6201729
ENSMUSG00000034739	Mfrp	0.33393231	−1.5823724	0.00052206	0.01229759	39.7498381	14.4999344	13.2737551	6.94579469
ENSMUSG00000031762	Mt2	0.32991896	−1.5998164	1.0548E-07	6.5725E-06	168.193072	36.616843	55.4900842	25.6080296
ENSMUSG00000041323	Ak7	0.32977503	−1.6004459	4.6104E-12	6.1713E-10	199.556069	21.9016896	65.8086098	34.3900865
ENSMUSG00000051029	Serpinb1b	0.32941754	−1.6020107	3.5974E-09	3.1062E-07	94.6752694	19.6879546	31.1876943	10.0230269
ENSMUSG00000048826	Dact2	0.32857889	−1.6056883	2.9565E-09	2.6061E-07	67.5667011	4.46401165	22.200992	5.13824377
ENSMUSG00000022342	Kcnv1	0.32508045	−1.6211313	1.7177E-20	5.4319E-18	199.990566	14.5393979	65.0130242	12.6451042
ENSMUSG00000054150	Syne3	0.3231294	−1.6298161	3.1021E-05	0.00111476	33.3875849	8.58598373	10.7885102	7.06796669
ENSMUSG00000031786	Drc7	0.32243301	−1.6329286	3.544E-06	0.00015813	85.4447152	23.245642	27.5501971	13.0218243
ENSMUSG00000052125	F730043M19Rik	0.32191534	−1.6352468	1.3558E-43	1.715E-40	836.211224	67.7734405	269.189218	39.8010956

(*Table continues*.)

Table 2. Continued

		Mutant vs control				Controls (FPKM)		Sufu-cKO (FPKM)	
Ensembl_ID	Gene	FC	Log2 FC	RawP	FDR	Average	SD	Average	SD
ENSMUSG00000051590	Map3k19	0.31584865	−1.6626947	9.5026E-07	4.9264E-05	42.4070608	5.46925196	13.3942131	5.98432819
ENSMUSG00000038756	Ttll6	0.31442691	−1.6692034	3.5542E-07	2.0026E-05	43.8239805	7.14725631	13.7794388	5.32505088
ENSMUSG00000037035	Inhbb	0.31304247	−1.6755697	3.5631E-13	5.6339E-11	1032.43414	183.884547	323.195732	101.081264
ENSMUSG00000061808	Ttr	0.30760456	−1.7008512	1.5449E-08	1.1495E-06	14304.5738	3188.63324	4400.15215	2002.44794
ENSMUSG00000101179	Gm29455	0.30577595	−1.7094531	0.00022723	0.00607588	22.0819173	3.56153377	6.75211929	4.45730172
ENSMUSG00000047230	Cldn2	0.30381703	−1.7187254	3.9887E-06	0.00017611	35.7538356	8.01693491	10.862624	4.88830751
ENSMUSG00000023411	Nfatc4	0.30062238	−1.7339757	4.2209E-32	3.4446E-29	2612.87821	255.642523	785.489668	211.063917
ENSMUSG00000052861	Dnah6	0.29886891	−1.7424153	3.1911E-28	2.1245E-25	273.455133	14.0180069	81.7272382	31.1194414
ENSMUSG00000079436	Kcnj13	0.29519998	−1.7602355	8.5729E-15	1.6186E-12	154.575354	22.3890493	45.6306411	19.5662979
ENSMUSG00000041380	Htr2c	0.29407271	−1.7657552	4.4479E-14	7.9244E-12	624.592196	97.9410461	183.675522	78.5388983
ENSMUSG00000036915	Kirrel2	0.29200719	−1.7759242	2.6849E-06	0.00012305	33.4634662	7.26910455	9.77157288	2.22998818
ENSMUSG00000052273	Dnah3	0.28765566	−1.7975852	4.7127E-05	0.00160682	25.2599583	3.67878464	7.26617003	3.75148251
ENSMUSG00000079644	Gm1110	0.28392892	−1.8163983	2.9746E-06	0.00013511	32.8774224	7.5375032	9.33485109	4.91024916
ENSMUSG00000026156	B3gat2	0.282786	−1.8222174	4.8209E-09	4.012E-07	579.450548	146.932197	163.860502	41.8508846
ENSMUSG00000026483	Fam129a	0.27079892	−1.8847061	7.0404E-37	6.8506E-34	503.603766	18.0076799	136.375357	59.7699859
ENSMUSG00000032057	4833427G06Rik	0.26931801	−1.8926174	1.765E-05	0.00068069	25.5824477	4.27928489	6.88981391	4.48211718
ENSMUSG00000053519	Kcnip1	0.26834904	−1.8978174	6.5085E-10	6.144E-08	524.826687	134.430748	140.836739	12.9116317
ENSMUSG00000095369	Gm21859	0.26507365	−1.9155348	8.173E-06	0.00033512	28.1379005	9.23471864	7.45861593	2.55505494
ENSMUSG00000028523	Tctex1d1	0.25973819	−1.9448699	9.051E-05	0.00279586	21.0867309	3.99476738	5.47702936	2.35731468
ENSMUSG00000053441	Adamts19	0.25950133	−1.9461861	3.797E-07	2.1158E-05	505.608463	158.402559	131.20607	17.3208447
ENSMUSG00000062939	Stat4	0.25712319	−1.9594684	1.7507E-13	2.9139E-11	224.471089	49.3166255	57.7167219	4.10100963
ENSMUSG00000027962	Vcam1	0.25534623	−1.9694734	8.0639E-61	2.0401E-57	2919.72302	248.427664	745.540259	144.812934
ENSMUSG00000062778	Chia1	0.25252559	−1.9854985	9.6048E-07	4.9691E-05	31.0658681	2.32254611	7.84492666	3.13891683
ENSMUSG00000032420	Nt5e	0.2485827	−2.0082022	4.238E-08	2.9483E-06	51.5234588	13.2304449	12.8078406	6.2866767
ENSMUSG00000059146	Ntrk3	0.24840437	−2.0092375	2.0583E-58	4.3394E-55	1208.03749	113.821023	300.081793	48.1219032
ENSMUSG00000016386	Mpped2	0.24535894	−2.0270342	7.0496E-41	7.7543E-38	12554.5568	1398.64186	3080.3728	705.541299
ENSMUSG00000025469	Msx3	0.24431404	−2.0331913	1.7266E-10	1.8125E-08	55.2965682	9.06241138	13.5097279	5.44464353
ENSMUSG00000059991	Nptx2	0.2428446	−2.0418947	3.0911E-28	2.1135E-25	331.436701	43.8543483	80.4876128	22.6196345
ENSMUSG00000004558	Ndrg2	0.24232547	−2.044982	4.0113E-16	8.7484E-14	5271.28886	1007.63586	1277.36755	400.771571
ENSMUSG00000066224	Arid3c	0.24020674	−2.0576515	4.5053E-07	2.4671E-05	32.6716593	9.81351364	7.84795274	3.93796433
ENSMUSG00000039672	Kcne2	0.23992137	−2.0593664	2.303E-14	4.1616E-12	860.829612	155.413044	206.531418	108.293694
ENSMUSG00000061802	Armc4	0.22863882	−2.1288577	1.7317E-06	8.313E-05	39.1832147	12.0476208	8.95880413	5.28814123
ENSMUSG00000037086	Prr32	0.22125882	−2.1761932	5.5796E-05	0.00185735	45.1412802	16.648903	9.98790625	8.18876702
ENSMUSG00000054855	Rnd1	0.21071589	−2.246629	2.3699E-49	3.331E-46	374.829696	36.6287339	78.9825744	9.05599108
ENSMUSG00000052629	Gm9885	0.20466141	−2.288689	8.194E-15	1.5586E-12	84.4762655	16.9287558	17.2890316	8.53422365
ENSMUSG00000026167	Wnt10a	0.18096541	−2.4662141	4.4178E-05	0.00151241	22.9061816	9.76492573	4.14522666	2.39657559
ENSMUSG00000020061	Mybpc1	0.12630398	−2.985028	3.8792E-24	1.7297E-21	83.546948	9.20468128	10.5523119	5.96083163
ENSMUSG00000048758	Rpl29	0.11675463	−3.0984484	0.00119128	0.02428541	205.380236	133.296103	23.9790929	7.41230562
ENSMUSG00000013766	Ly6g6e	0.11025929	−3.1810278	4.1587E-06	0.00018203	22.2315421	9.62724081	2.45123409	0.92301324
ENSMUSG00000023484	Prph	0.06998924	−3.8367231	3.7796E-07	2.1108E-05	49.6871139	22.4248732	3.47756316	4.30497059
ENSMUSG00000004892	Bcan	0.06566811	−3.9286633	2.6431E-13	4.3141E-11	438.508098	149.646904	28.795998	17.7145662
ENSMUSG00000022129	Dct	0.04634385	−4.4314784	2.6101E-82	1.3206E-78	1257.91335	175.303114	58.296544	14.7646366
ENSMUSG00000062353	Gm15772	0.00636491	−7.2956441	3.0176E-08	2.175E-06	419.758154	278.168105	2.67172295	1.22642389
ENSMUSG00000083773	Gm13394	0.00469112	−7.7358528	5.4181E-09	4.4217E-07	1387.75004	923.084254	6.51009789	1.4542309

[a]The top significantly expressed genes (FDR < 0.05) with a Log2FC of ±1.5; and read counts (FPKM) >20 for at least 1 genotype group in the E12.5 Sufu-cKO dorsal forebrain ($n = 4$ per genotype). FC, Unlogged fold change; Log2FC, log2 fold change; RawP, unadjusted p value; FDR, p value adjusted for multiple comparisons; average FPKM, average normalized sample values; SD, standard deviation of normalized sample values.

Protein (*Hhip*), are specifically upregulated in the E12.5 Sufu-cKO neocortex compared with controls (FDR < 0.01; Fig. 2*B*; Table 3). We validated these observations by ISH using probes for *Ptch1*, which was ectopically expressed throughout the neocortical expanse (Fig. 2*E*,*F*) in contrast to controls (Fig. 2*C*,*D*). Levels of *Ptch1* expression were confined within the VZ/SVZ across the cortical and hippocampal primordia (Fig. 2*G*,*H*) and were particularly high in rostral neocortical regions. Interestingly, expression of *Ptch1* also followed a visible columnar pattern (Fig. 2*G*,*H*, arrows) along the anterior neocortex of the E12.5 Sufu-cKO mice. These findings indicated deregulation of SHH signaling in discrete neocortical progenitor subpopulations, and not differentiated neurons, in the E12.5 neocortex of Sufu-cKO mice.

Altered molecular identity of progenitors in the E12.5 Sufu-cKO neocortex

Since changes in SHH signaling activity in the neocortex are known to disrupt progenitor fate specification in late-stage corticogenesis (Komada et al., 2008a; L. Wang et al., 2016), we wondered whether the ectopic activation of SHH signaling at E12.5 initiated a cascade of disruptive differentiation events. Functional analysis of the transcriptome using the Database for Annotation, Visualization, and Integrated Discovery (DAVID; https://david.ncifcrf.gov/) (Huang et al., 2009) found overrepresentation of genes with gene ontology terms associated with neural development, commitment, specification, and differentiation (Fig. 3*A*). Further examination of specific gene sets showed relatively mild changes in the expression of genes typical of dorsal

Table 3. Expression of genes associated with the SHH signaling pathway[a]

		Mutant vs control				Control (FPKM)		Sufu-cKO (FPKM)	
Ensembl_ID	Gene	FC	Log2 FC	RawP	FDR	Average	SD	Average	SD
ENSMUSG00000023000	Dhh	0.60	−0.74	3.42E-01	1.00E + 00	5.67	0.89	3.40	3.13
ENSMUSG00000006538	Ihh	1.19	0.25	8.40E-01	1.00E + 00	4.16	1.44	4.93	2.29
ENSMUSG00000002633	Shh	1.04	0.06	1.00E + 00	1.00E + 00	0.22	0.43	0.23	0.45
ENSMUSG00000025407[b]	Gli1	18.64	4.22	3.99E-198	1.01E-193	81.59	30.43	1520.57	123.98
ENSMUSG00000048402[b]	Gli2	1.57	0.65	3.41E-11	4.02E-09	2180.65	129.32	3420.06	273.85
ENSMUSG00000021318	Gli3	1.06	0.08	4.29E-01	1.00E + 00	10140.19	580.10	10701.03	996.24
ENSMUSG00000021466[b]	Ptch1	10.50	3.39	5.01E-57	8.45E-54	692.64	117.33	7274.61	1053.61
ENSMUSG00000028681[b]	Ptch2	10.64	3.41	1.59E-70	6.69E-67	52.63	16.71	559.98	68.00
ENSMUSG00000064325[b]	Hhip	82.08	6.36	6.07E-54	9.03E-51	8.92	2.88	732.06	155.71
ENSMUSG00000022687	Boc	0.98	−0.03	7.09E-01	1.00E + 00	4082.93	354.37	3985.87	387.16
ENSMUSG00000052957[b]	Gas1	0.61	−0.71	1.86E-06	8.88E-05	7965.08	1277.51	4860.73	187.79
ENSMUSG00000038119[b]	Cdon	0.43	−1.23	4.91E-26	2.70E-23	21912.76	2371.76	9314.91	711.74
ENSMUSG00000001761	Smo	0.92	−0.12	2.02E-01	9.02E-01	5502.55	145.38	5069.64	584.69
ENSMUSG00000025231[b]	Sufu	0.36	−1.46	7.48E-46	9.96E-43	3436.77	291.10	1248.15	144.31

[a]FC, Unlogged fold change; Log2FC, log2 fold change; RawP, unadjusted *p* value; FDR, *p* value adjusted for multiple comparisons; average FPKM, average normalized sample values; SD, standard deviation of normalized sample values.
[b]Genes are significantly upregulated in the E12.5 Sufu-cKO dorsal forebrain ($n = 4$ mice per genotype).

forebrain progenitors (Fig. 3*B*; Table 4). Indeed, similar to Pax6 expression in Figure 1, other markers for dorsal forebrain cells, such as *Tbr2*, *Lhx2*, and *Nr2f1*, remained expressed, and may be even expressed at slightly higher levels in the mutant neocortex as observed with *Pax6*, *Tbr1*, *Nr2f1*, or *Nr2f2* (Fig. 3*B*; Table 4). These findings validated the efficiency of the dissection and confirmed that the molecular identity of dorsal forebrain domains was established in the E12.5 Sufu-cKO neocortex.

Nevertheless, RNA levels for several ventral progenitor genes dramatically increased in the E12.5 Sufu-cKO neocortex compared with controls (Fig. 3*B*). We found a specific increase in the expression of subpallial-specific genes in the neocortex (Fig. 3*B*; Table 4). Moreover, while we previously did not observe a significant increase in Ascl1 protein expression in the E12.5 neocortex (Yabut et al., 2015), here we found significantly higher levels of Ascl1 transcript, despite not detecting Ascl1 protein (Extended Data Fig. 3-1*A*). Additionally, significant upregulation of genes normally expressed in the GE, such as *Gsx2* and *Dlx1/2* (Petryniak et al., 2007), was also ectopically expressed in the neocortex of E12.5 Sufu-cKO mice (Fig. 3*B*).

We subsequently conducted immunostaining or ISH experiments to validate the expression of subpallial-specific markers. In agreement with the transcript increase quantified by RNA-Seq, visibly higher levels of $Tbr2^+$, $NR2F1^+$, and $Lhx2^+$ cells were observed across the anterior to posterior axis of the Sufu-cKO neocortex compared with controls (Fig. 3*B*,*C*; Extended Data Fig. 3-1*B*,*C*). Similarly, ectopic expression of subpallial-specific genes Olig2, Dlx1, and Gsx1 was detected in the E12.5 Sufu-cKO neocortex (Fig. 3*D*,*E*; Extended Data Fig. 3-1*D*). Expression of these genes was detected in the SVZ and VZ regions of the E12.5 Sufu-cKO neocortex and exhibited a columnar pattern, whereas these genes were absent in controls. Additionally, neocortical progenitors in these regions were improperly specified since we detected ectopic expression of the ventral forebrain progenitor marker, Olig2, in areas where Pax6 was absent in the E12.5 Sufu-cKO neocortex (Fig. 3*F*, arrows), whereas Olig2 was completely absent in the neocortex of control mice. This expression pattern persisted in the anterior regions of the E14.5 Sufu-cKO neocortex but not in posterior regions (Extended Data Fig. 3-2*A*). However, we did not see similarly extensive disruptions in Tbr2 expression in the E12.5 Sufu-cKO neocortex, even in areas where $Olig2^+$ cells were highly enriched (Fig. 3*C*,*G*). Nevertheless, while the majority of $Tbr2^+$ cells in the E12.5 Sufu-cKO SVZ did not coexpress Olig2, a few cells within the VZ coexpressed Olig2 and Tbr2 (Fig. 3*G*, boxed inset, arrowheads). Further, by E14.5, $Tbr2^+$ cells, similar to $Pax6^+$ cells, became intermittent in the anterior neocortex of Sufu-cKO mice and were populated by $Ascl1^+$ cells (Extended Data Fig. 3-2*B*,*C*). Ectopic expression of Olig2 was not prevalent in the E11.5 Sufu-cKO neocortex, although we noted irregularities in Olig2 expression near the pallial-subpallial boundary (Extended Data Fig. 3-1*E*), indicating that a subset of aberrant progenitors may be present at this stage. Together, these findings establish that activation of SHH signaling in early stages of corticogenesis did not disrupt the regionalization of dorsoventral axis but has begun to destabilize the specification program of neocortical RG progenitors to disrupt the specification of $Tbr2^+$ IPCs.

Ectopic activation of SHH signaling upregulates FGF15 expression

To determine how these genetic changes mediated specification defects in the E12.5 Sufu-cKO neocortex, we further analyzed the overall nature of differentially expressed genes from our RNA-Seq data (Table 2). Functional analysis of the transcriptome using DAVID showed enrichment of genes encoding proteins with roles in cell-cell communications, such as membrane-bound or extracellular matrix proteins in the E12.5 Sufu-cKO transcriptome (Fig. 4*A*; Table 5). Thus, the molecular makeup of the VZ/SVZ progenitor niche has been significantly altered in response to the ectopic activation of SHH signaling in the E12.5 Sufu-cKO neocortex. Among these is the gene encoding the secreted ligand, *Fibroblast Growth factor 15* (*Fgf15*) (Fig. 4*B*). *Fgf15* was a previously reported SHH signaling gene target in the developing cerebellum affecting neuronal precursor behavior (Gimeno and Martinez, 2007; Komada et al., 2008b; Kim et al., 2018). Similarly, we found that, in the E12.5 Sufu-cKO neocortex, *Fgf15* dramatically increased (5.72 log2 fold change, $p < 0.0001$), likely as a consequence of Gli3R loss. ISH using *Fgf15* riboprobes confirmed these findings, with *Fgf15* ectopically expressed throughout the neocortical wall of the E12.5 and E14.5 Sufu-cKO mice while *Fgf15* expression was relatively low in controls

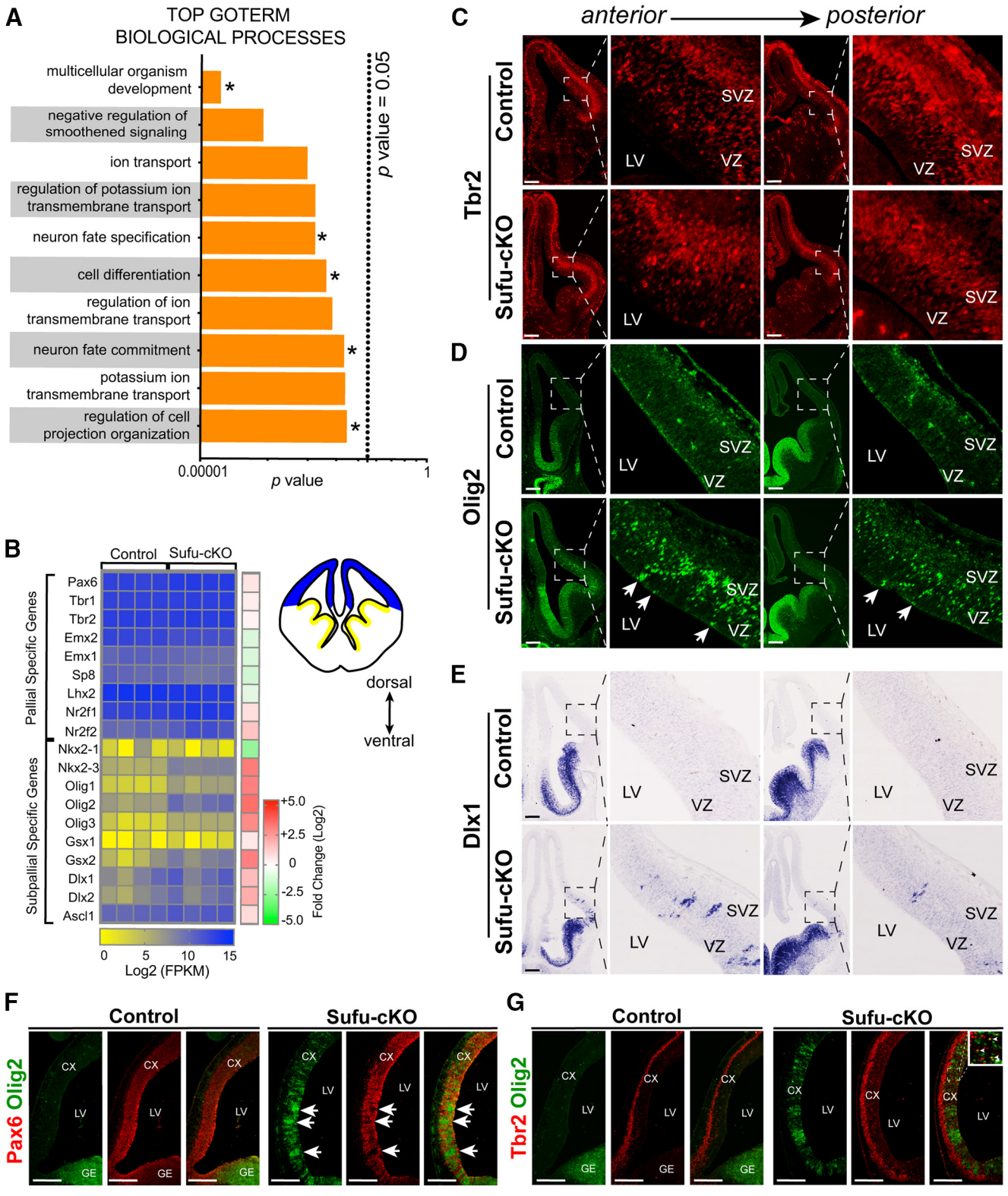

Figure 3. Increased expression of ventral progenitor markers in neocortical progenitors of E12.5 Sufu-cKO embryos. ***A***, Functional annotation of differentially expressed genes identified by RNA-Seq show top GOTERM Biological Processes (with adjusted p value < 0.05) involve development, specification, differentiation, and fate commitment (*). There is also a notable enrichment in ion transmembrane transport GOTERMs, reflecting disrupted electrophysiological properties because of abnormal differentiation of neurons or specific neuronal subtypes. ***B***, Heat map of select genes typically expressed by dorsal or ventral progenitors in individual control and Sufu-cKO mice ($n = 4$ mice per genotype). RNA levels (Log2 FPKM scale) reflect mild differences in expression of dorsal progenitor genes (reflected by fold change scale), while dramatic differences in expression levels of ventral progenitor genes are observed between controls and Sufu-cKO dorsal forebrain (see also Table 4). ***C***, Immunofluorescence staining for pallial-specific marker, Tbr2, in coronal sections of the E12.5 Sufu-cKO and control forebrain showed exclusive expression in the neocortex across the A-P axis. Pallial-specific markers NR2F1 and Lhx2 were similarly confined in the dorsal forebrain (Extended Data Fig. 3-1*B*,*C*). Scale bar, 100 µm. ***D***, ***E***, Immunofluorescence staining for Olig2 (***D***) and ISH for Dlx1 (***E***) on coronal sections of the E12.5 control and Sufu-cKO forebrain validate the ectopic expression of subpallial-specific genes across the A-P axis of the E12.5 Sufu-cKO neocortex, whereas these genes were absent in controls. Olig2- and Dlx1- expressing cells largely localized in the VZ and SVZ. Some groups of cells expressing

Table 4. Expression of pallial- and subpallial-specific genes[a]

			Mutant vs control				Controls (FPKM)		Sufu-cKO (FPKM)	
	Ensembl_ID	Gene	FC	Log2 FC	RawP	FDR	Average	SD	Average	SD
Pallial-specific genes	ENSMUSG00000027168	Pax6	1.45178268	0.53782551	1.004E-08	7.6972E-07	7334.1262	557.776073	10647.5574	579.137216
	ENSMUSG00000035033	Tbr1	1.22502496	0.29281114	0.00215728	0.03954861	7034.87917	270.071078	8617.90254	557.7091
	ENSMUSG00000032446	Eomes	1.09461657	0.1304256	0.15380485	0.79883164	8778.80064	946.263097	9609.42061	765.318
	ENSMUSG00000043969	Emx2	0.60690796	−0.7204503	1.1807E-13	2.0184E-11	6169.69045	604.010197	3744.43426	268.720823
	ENSMUSG00000033726	Emx1	0.60444715	−0.7263119	3.255E-06	0.00014653	1588.14413	187.604638	959.9492	200.078024
	ENSMUSG00000048562	Sp8	0.53768597	−0.8951643	0.00018879	0.00520849	1437.66797	300.580706	773.01389	199.878775
	ENSMUSG00000000247	Lhx2	0.70189749	−0.5106678	6.8017E-08	4.4235E-06	17739.2767	1437.7177	12451.1537	1359.0387
	ENSMUSG00000069171	Nr2f1	1.59051974	0.66949828	0.00014645	0.00415822	7171.74849	888.316712	11406.8075	2022.77936
	ENSMUSG00000030551	Nr2f2	2.62720361	1.39352802	0.00048355	0.01154083	1231.1201	229.798831	3234.40319	1174.67098
Subpallial-specific genes	ENSMUSG00000041911	Dlx1	3.09901298	1.6318088	0.07970986	0.56981627	461.094387	506.237194	1428.93749	954.933235
	ENSMUSG00000023391	Dlx2	3.95059159	1.98206871	0.02352951	0.25117012	184.932474	200.493153	730.592677	453.539091
	ENSMUSG00000020052	Ascl1	1.72359337	0.78541945	0.00107784	0.02236943	1331.20054	187.629663	2294.44843	561.105261
	ENSMUSG00000053129	Gsx1	1.35616481	0.43953252	0.85642916	1	2.18572234	4.37144469	2.96419973	2.64163128
	ENSMUSG00000035946	Gsx2	9.19782474	3.20129271	8.7129E-05	0.00271461	40.8981257	51.8805517	376.173792	198.118943
	ENSMUSG00000046160	Olig1	9.35940117	3.22641623	4.6615E-09	3.905E-07	6.21737577	1.93182166	58.1909141	21.2357905
	ENSMUSG00000039830	Olig2	12.6102384	3.65652365	2.65E-10	2.7033E-08	69.5186604	19.2058548	876.646882	335.706
	ENSMUSG00000045591	Olig3	7.20471446	2.84894125	8.3417E-12	1.0658E-09	5.25145549	3.63879005	37.8352373	3.88669789
	ENSMUSG00000001496	Nkx2-1	0.22177988	−2.1727996	0.39910601	1	25.2811711	45.3686169	5.6068551	6.573452
	ENSMUSG00000044220	Nkx2-3	10.1453116	3.34274127	7.382E-20	2.1222E-17	34.6890788	7.47294372	351.931514	86.7310817

[a]Expression of select genes typically expressed by dorsal or ventral progenitor in individual control and Sufu-cKO mice ($n = 4$ mice per genotype). FC, Unlogged fold change; Log2FC, log2 fold change; RawP, unadjusted p value; FDR, p value adjusted for multiple comparisons; average FPKM, average normalized sample values; SD, standard deviation of normalized sample values.

(Fig. 4*C*,*D*). We also observed upregulation of *Fgf15* in embryos in which Smo was constitutively active in neocortical progenitors (*Emx1-Cre;SmoM2* or SmoM2-cA) (Long et al., 2001), confirming the role of activated SHH signaling in inducing *Fgf15* gene expression in the embryonic neocortex (Extended Data Fig. 4-1). Importantly, *Fgf15* expression in the E12.5 Sufu-cKO was detected along the VZ/SVZ, and particularly overlapped with *Ptch1*-expressing cells in the VZ (Fig. 4*E*). These observations indicated that ectopic *Fgf15* expression was induced in RG progenitors along the VZ and persisted in IPCs as a consequence of loss of Sufu and deregulated SHH signaling.

Upregulated FGF15 expression correlates with ectopic activation of MAPK signaling in neocortical progenitor zones

FGF15 preferentially binds to its cognate receptor, FGF receptor 4 (FGFR4), to activate intracellular signaling cascades, particularly the Ras/mitogen-activated protein kinase (MAPK) pathway (Guillemot and Zimmer, 2011). Indeed, in the neocortex of E12.5 Sufu-cKO mice, MAPK signaling pathway activity, as marked by phosphorylated-ERK1/2 (pERK1/2$^+$) labeling, is visibly upregulated unlike controls (Fig. 5*A*). We found that pERK1/2$^+$ areas occupied the progenitor-rich VZ/SVZ neocortical regions, whereas it was largely undetected in similar neocortical regions in controls. Quantification of pERK1/2$^+$ regions in representative sections across the dorsal forebrain (Fig. 5*C*) showed a consistently larger area with pERK1/2$^+$ immunoreactivity in the E12.5 Sufu-cKO cortex compared with controls (two-way ANOVA, $p = 0.0365$, $n = 5$ control/Sufu-cKO embryos) (Fig. 5*D*; Table 1). This remained true at E14.5, where pERK1/2$^+$-rich regions were detected further toward the dorsal regions of the Sufu-cKO neocortex (Fig. 5*B*). Quantification of pERK1/2$^+$ regions in the E14.5 neocortex confirmed these observations and showed a significant increase in Sufu-cKO mice (two-way ANOVA, $p = 0.013$, $n = 3$-5 control/Sufu-cKO embryos) (Fig. 5*E*; Table 1). At both E12.5 and E14.5 time points, cells labeled with pERK1/2$^+$ clearly overlapped with FGF15-expressing VZ/SVZ areas in the Sufu-cKO neocortex (Fig. 4*D*). Together, these observations indicated that loss of Sufu resulted in the overexpression of FGF15 in the neocortex, subsequently driving the ectopic activation of FGF signaling to activate intracellular MAPK signaling in neocortical progenitors.

FGF15 upregulation is required to elicit SHH signaling-mediated defects in the production and specification of IPCs

Reduction in IPCs is a consistent phenotype in the embryonic neocortex of mice with excessive levels of SHH signaling, including Sufu-cKO mice (Komada et al., 2008a; Dave et al., 2011; Yabut et al., 2015). We therefore investigated whether downregulation of IPCs in the neocortex because of ectopic SHH signaling is directly mediated by FGF15 signaling. To test this, we cultured WT forebrain slices from the anterior regions of E12.5 control and Sufu-cKO embryos (Fig. 6*A*). Forebrain organotypic cultures maintain the 3D structure of the VZ/SVZ niche, allowing for careful examination of how precisely added compounds affect progenitor behavior over time. Forebrain slices cultured for

←

Olig2 and Dlx1 also appeared in columnar arrangement (arrows). Similar columnar pattern was also detected in cells ectopically expressing another subpallial-specific marker, Gsx2 (Extended Data Fig. 3-1*D*). Few Olig2$^+$ cells also began to exhibit an irregular pattern along the pallial-subpallial boundary in the E11.5 Sufu-cKO forebrain (Extended Data Fig. 3-1*E*). Scale bar, 100 μm. ***F***, Double immunofluorescence staining on E12.5 sagittal sections with Pax6 and Olig2 showed ectopic expression of Olig2 in areas where Pax6 is missing in the Sufu-cKO neocortex (arrows), whereas Olig2 was not expressed in this region in the control neocortex. However, Ascl1 was not similarly affected since protein levels of Ascl1 were low in the E12.5 Sufu-cKO and control neocortex (Extended Data Fig. 3-1*A*). This pattern of Olig2 and Pax6 expression continued in the E14.5 neocortex, when ectopic expression of Ascl1 was also prevalent in the VZ/SVZ (Extended Data Fig. 3-2*A*,*B*). Scale bar, 250 μm. ***G***, Double immunofluorescence staining with Tbr2 and Olig2 on sagittal sections of E12 Sufu-cKO and control littermates showed that, unlike Pax6$^+$ cells, the distribution of Tbr2$^+$ cells was not affected in the anterior regions where ectopic expression of Olig2 was present. However, Tbr2$^+$ cells were found to coexpress Olig2 in more anterior regions of the E12.5 Sufu-cKO neocortex. By E14.5, areas where Tbr2$^+$ cells were absent in the anterior neocortex, showed Ascl1-expressing cells (Extended Data Fig. 3-2*C*). Scale bar, 250 μm.

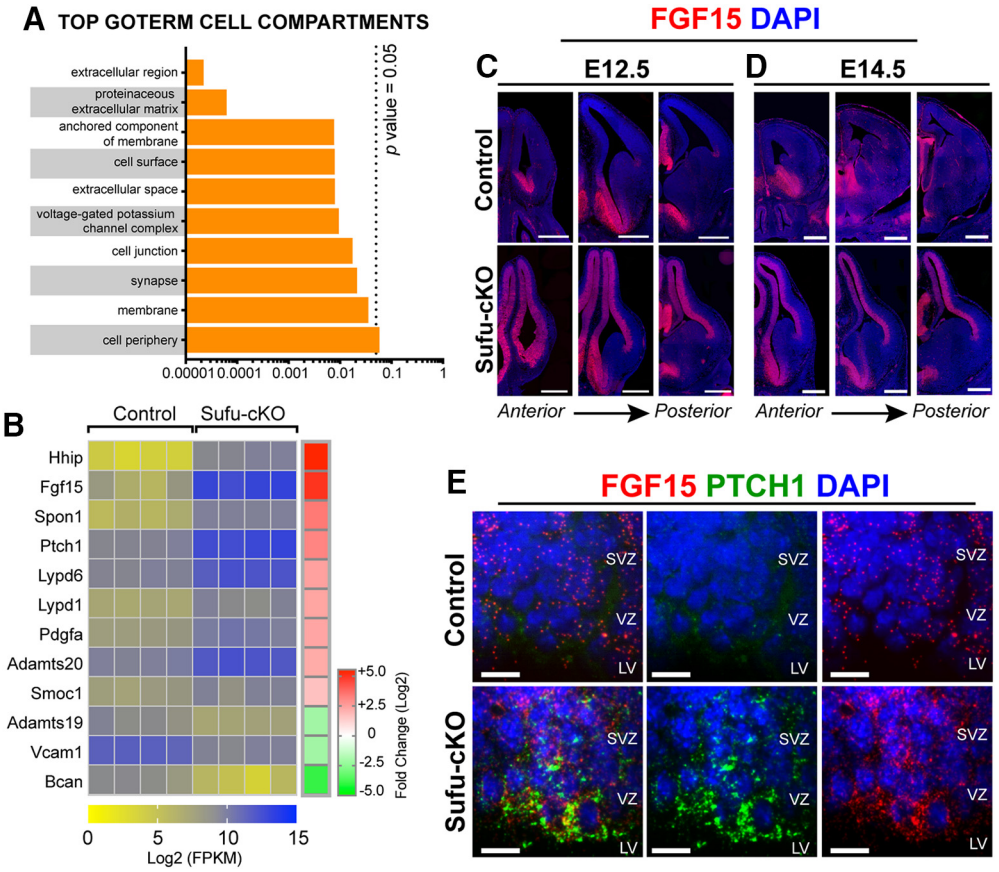

Figure 4. Ectopic activation of SHH signaling drives Fgf15 expression in neocortical progenitors of E12.5 Sufu-cKO embryos. ***A***, Functional annotation of differentially expressed genes identified by RNA-Seq showing the majority of genes encode proteins that localize to extracellular matrix or cell surface/membrane as the top GOTERMs cell compartments (with adjusted *p* value < 0.05). ***B***, Heat map of top differentially expressed genes encoding extracellular matrix or cell membrane-bound proteins between control and Sufu-cKO mice ($n = 4$ mice per genotype). RNA levels (Log2 FPKM scale) show expression of *Fgf15* is significantly upregulated (reflected by fold change scale in the E12.5 Sufu-cKO dorsal forebrain; see also Table 5). ***C***, ***D***, ISH for *Fgf15* in the E12.5 and E14.5 control and Sufu-cKO neocortex. High levels of *Fgf15* expression were detected throughout the E12.5 Sufu-cKO dorsal forebrain, and particularly enriched in the VZ/SVZ regions, whereas *Fgf15* expression was detected only in ventral forebrain regions in controls (***C***). Expression of *Fgf15* persisted in the E14.5 control and Sufu-cKO forebrains (***D***). Ectopic expression of *Fgf15* was also detected in transgenic mice carrying constitutively active Smoothened allele (Extended Data Fig. 4-1). These findings confirmed that activation of SHH signaling and loss of Sufu force Fgf15 expression in the embryonic neocortex. Scale bar, 500 μm. ***E***, Multiplex RNAscope ISH of Ptch1 and Fgf15 riboprobes on E12.5 brains did not detect Ptch1 expression, whereas low levels of Fgf15 expression were detected in the VZ and SVZ of the neocortex of controls. In the E12.5 Sufu-cKO neocortex, high levels of Ptch1 and Fgf15 colocalization were detected in the VZ and SVZ. Sections are counterstained with DAPI. Scale bar, 10 μm.

Table 5. List of genes encoding extracellular matrix or cell membrane-bound proteins[a]

		Mutant vs control				Controls (FPKM)		Sufu-cKO (FPKM)	
Gene	Description	FC	Log2 FC	RawP	FDR	Average	SD	Average	SD
Hhip	Hedgehog-interacting protein	82.0823811	6.35900068	6.07E-54	9.03E-51	8.91857894	2.87906586	732.058195	155.710915
Fgf15	FGF15	52.7038764	5.71983717	1.38E-96	1.16E-92	152.277335	111.900656	8025.60586	1237.95433
Spon1	spondin 1, (f-spondin) extracellular matrix protein	14.9532123	3.90238353	2.55E-158	3.23E-154	56.2092056	22.9496826	840.508183	67.3977619
Ptch1	patched homolog 1	10.5027097	3.39268968	5.01E-57	8.45E-54	692.640882	117.331353	7274.60609	1053.60989
Lypd6	LY6/PLAUR domain containing 6	6.23322426	2.63997862	3.73E-23	1.55E-20	714.738273	124.510077	4455.12394	879.153524
Lypd1	Ly6/Plaur domain containing 1	5.78045668	2.53118348	1.68E-14	3.08E-12	108.297771	11.4653093	626.010575	155.439255
Pdgfa	platelet derived growth factor, alpha	5.60936415	2.48783724	8.41E-17	1.95E-14	213.357738	41.0886507	1196.80125	267.580448
Adamts20	a disintegrin-like and metallopeptidase (reprolysin type) with thrombospondin Type 1 motif, 20	5.09486349	2.34904349	8.48E-35	7.66E-32	879.123707	153.586556	4479.01527	645.467259
Smoc1	SPARC related modular calcium binding 1	3.28121386	1.71422963	5.24E-06	0.00022471	195.520108	59.5128888	641.543288	199.481655
Adamts19	a disintegrin-like and metallopeptidase (reprolysin type) with thrombospondin Type 1 motif, 19	0.25950133	−1.9461861	3.80E-07	2.12E-05	505.608463	158.402559	131.20607	17.3208447
Vcam1	vascular cell adhesion molecule 1	0.25534623	−1.9694734	8.06E-61	2.04E-57	2919.72302	248.427664	745.540259	144.812934
Bcan	brevican	0.06566811	−3.9286633	2.64E-13	4.31E-11	438.508098	149.646904	28.795998	17.7145662

[a]Top differentially expressed genes encoding extracellular matrix or cell membrane-bound proteins between the E12.5 control and Sufu-cKO dorsal forebrain ($n = 4$ embryos per genotype). FC, Unlogged fold change; Log2FC, log2 fold change; RawP, unadjusted *p* value; FDR, *p* value adjusted for multiple comparisons; average FPKM, average normalized sample values; SD, standard deviation of normalized sample values.

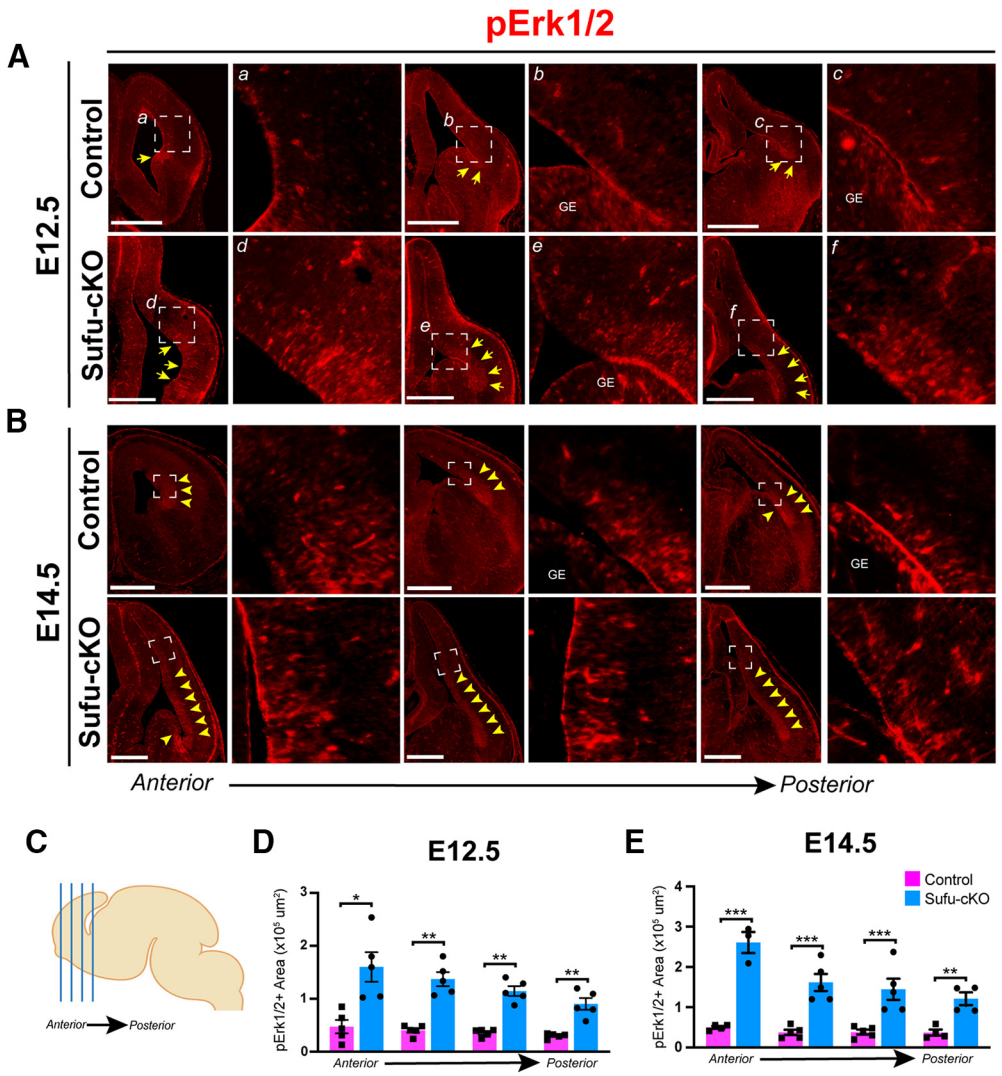

Figure 5. Upregulated FGF15 expression correlates with ectopic activation of MAPK signaling in neocortical progenitor zones. ***A***, ***B***, Immunofluorescence staining against phosphorylated Erk1/2 (pErk1/2) was conducted on E12.5 and E14.5 control and Sufu-cKO brains to detect for MAPK signaling activation. pErk1/2-expressing cells (pErk1/2$^+$) were detected along the pallial-subpallial boundary (PSB) of the E12.5 control and Sufu-cKO forebrain (white arrows). However, pErk1/2$^+$ cells were found from the PSB and the lateral cortex, particularly in the VZ/SVZ regions (yellow arrows, ***A***). At E14.5, pErk1/2$^+$ cells expanded dorsally within the VZ/SVZ regions in both control and Sufu-cKO neocortex (***B***). However, pErk1/2$^+$ cells in the Sufu-cKO neocortex greatly expanded compared with controls (yellow arrows). Scale bars: 500 μm (***A***,***B***). ***C–E***, Four representative sections across the A-P axis of the forebrain (***C***) were sampled to measure pERK1/2$^+$ regions in the E12.5 and E14.5 control and Sufu-cKO mice. Bar graphs of quantification of pErk1/2$^+$ regions in the neocortex of E12.5 (***D***) and E14.5 (***E***) control and Sufu-cKO mice ($n = 3$-5 embryos per genotype) represent significant interaction between position and genotype (repeated-measures two-way ANOVA, $p = 0.0365$). Significance between genotypes in Ph-Erk1/2$^+$ regions in the Sufu-cKO neocortex at both E12.5 and E14.5, particularly in anterior regions: $^*p \leq 0.05$; $^{**}p \leq 0.01$; $^{***}p \leq 0.001$; repeated-measures, two-way ANOVA with Holm-Sidak's multiple comparisons test. Values of statistics are shown in Table 1. Bar graphs represent average values. Error bars indicate SEM.

2 DIV maintain their anatomic features with well-preserved dorsal and ventral domains. Neocortical IPCs typically expressing Tbr2 (Hevner, 2019) were exclusively observed in the dorsal forebrain whereas ventral forebrain progenitors were typically expressing Olig2 (Miyoshi et al., 2007) (Fig. 6*B*). Addition of various compounds altered IPC numbers in neocortical regions of forebrain slices (one-way ANOVA, $p = 0.0001$, $n = 3$ per treatment condition) (Fig. 6*C*,*D*). SHH ligands significantly decreased the number of Tbr2$^+$ cells in neocortical slices after 2 DIV compared with mock-treated controls (SHH-treated = 3792 ± 913.9 cells/mm^2; DMSO-treated = 9207 ± 303.5 cells/mm^2; Holm-Sidak's multiple comparisons test, $p = 0.0004$). Similarly, Tbr2$^+$ IPCs were significantly reduced on addition of FGF15 alone (FGF15-treated = 6448 ± 526.8 cells/mm^2; Holm-Sidak's multiple comparisons test, $p = 0.05$) or with SHH (FGF15+ SHH-treated = 4511 ± 645.7 cells/mm^2; Holm-Sidak's multiple comparisons test, $p = 0.0014$). However, addition of cyclopamine, which inhibits SHH signaling by rendering Smo inactive, did not alter the number of Tbr2$^+$ IPCs (cyclopamine-treated = 8736 ± 644 cells/mm^2; Holm-Sidak's multiple comparisons test, $p = 0.6585$). Instead, addition of cyclopamine and FGF15 significantly reduced the number of IPCs after 2 DIV (cyclopamine + FGF15-treated = 5550 ± 187.3 cells/mm^2; Holm-Sidak's multiple comparisons test, $p = 0.0095$). These findings indicated that blocking transmembrane proteins upstream of the SHH signaling pathway cannot sufficiently alter IPC production. Additionally, expression of downstream SHH gene targets, particularly FGF15, is required to exert changes in neocortical IPCs of the developing neocortex.

High levels of FGF15 alter the specification program of neocortical progenitors

Ectopic SHH signaling in the developing neocortex ultimately results in the production of confused progenitors unable to

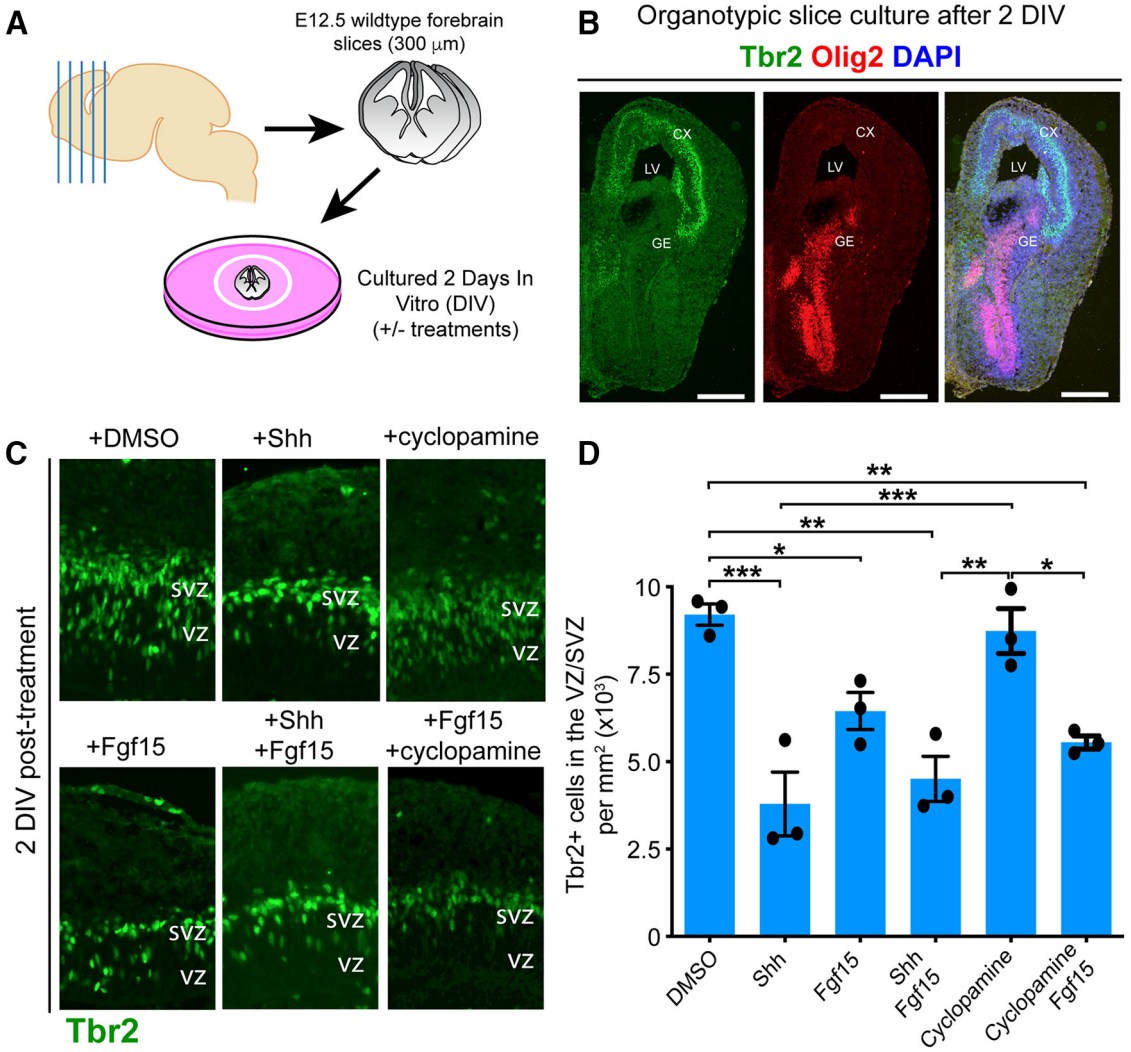

Figure 6. SHH signaling activates FGF15 signaling to inhibit production of neocortical IPCs. ***A***, Diagram of experimental design for organotypic forebrain slice cultures from WT E12.5 brains. ***B***, Immunofluorescence staining for dorsal (Tbr2, green) and ventral (Olig2, red) forebrain markers show exclusive localization of Tbr2-expressing and Olig2-expressing cells in dorsal and ventral forebrain regions, respectively. Merged images represent no overlap in Tbr2 or Olig2 labeling. Scale bar, 500 μm. ***C***, Immunofluorescence staining with Tbr2 of sectioned organotypic slice cultures fixed after 2 DIV. Slices treated with 200 ng/ml SHH and 100 ng/ml FGF15 show reduced numbers of $Tbr2^+$ IPCs compared with slices treated with DMSO or 5 μM cyclopamine. Combined FGF15 and SHH or FGF15 and cyclopamine also show reduced $Tbr2^+$ IPCs. Quantification of $Tbr2^+$ cells per unit area (***D***) confirm significant interaction between treatments (repeated-measures two-way ANOVA, $p = 0.0001$). Significant differences in $Tbr2^+$ IPCs in SHH and FGF15-treated slice cultures ($n = 3$ experiments [2 or 3 slices each experiment] per treatment condition). Significance between treatment conditions: $^*p \leq 0.05$; $^{**}p \leq 0.01$; $^{***}p \leq 0.001$; repeated-measures, one-way ANOVA with Holm-Sidak's multiple comparisons test. Values of statistics are shown in Table 1. Bar graphs represent average values. Error bars indicate SEM.

maintain a specified neocortical neural fate (Yabut et al., 2015). The expansive ectopic activation of MAPK signaling, capable of altering neocortical progenitor fate (Y. Wang et al., 2012), in the Sufu-cKO embryonic neocortex is a likely consequence of increasing levels of FGF15. We tested this by adding FGF15 in organotypic forebrain cultures and examined whether this alone altered the fate of neocortical progenitors based on Olig2 expression. Indeed, we found that, after 2 DIV, the decrease in $Tbr2^+$ IPCs correlated with an obvious increase in $Olig2^+$ cells in FGF15-treated slices compared with DMSO-treated controls (Fig. 7*A-D*). Further, low levels of Olig2 expression were detected in the VZ region, where Olig2 is typically not expressed in controls. Rather, in FGF15-treated slices, $Olig2^+$ cells may coexpress low levels of Tbr2, indicating that treatment of FGF15 began to alter the identity of RG progenitors transitioning into IPCs (Fig. 7*G*,*H*, arrows). Indeed, many $Olig2^+$ cells in the SVZ also expressed Tbr2 in FGF15-treated slices compared with DMSO-treated controls (Fig. 7*E*,*F*). Our quantification confirmed these observations, showing the ~4.5-fold increase in misspecified $Tbr2^+$ cortical progenitors in FGF15-treated slices compared with DMSO-treated controls (FGF15-treated = 18.2 ± 4.8 cells/mm^2; DMSO-treated = 4.03 ± 1.6 cells/mm^2; unpaired *t* test, $p = 0.0186$) (Fig. 7*I*). These findings indicate that excessive levels of FGF15 can sufficiently alter the identity of neocortical progenitors, leading to the failure to maintain a proper specification program in the developing neocortex.

Discussion

Excitatory neurons in the mammalian neocortex are generated in a limited period at embryonic stages and mature into molecularly diverse subpopulations at postnatal stages. A strict

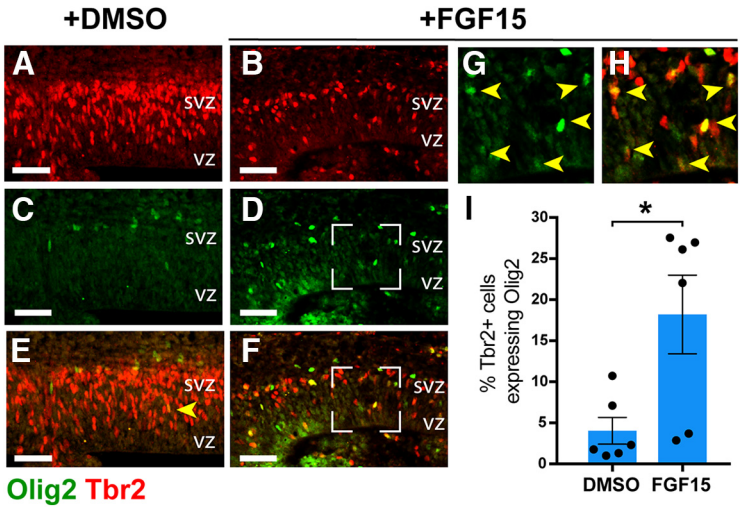

Figure 7. Increasing FGF15 levels alter the specification program of neocortical progenitors. ***A–F***, Double immunofluorescence staining with IPC marker Tbr2 (red) and the ventral progenitor marker Olig2 (green) on organotypic slice cultures fixed 2 DIV and after treatment. DMSO-treated slices show an abundance of $Tbr2^+$ IPCs in the SVZ (***A***) and some Olig2-expressing cells outside of the VZ/SVZ area (***B***). In contrast, $Tbr2^+$ IPCs in FGF15-treated slices are fewer (***B***) and more $Olig2^+$ cells are present in the VZ/SVZ (***F***). Although $Tbr2^+$ cells expressing Olig2 were also sometimes observed in DMSO-treated slices (yellow arrow, ***C***), the amount of double-labeled in FGF15-treated slices were visibly higher in the VZ/SVZ (***G***,***H***, yellow arrows). Scale bar, 50 μm. ***I***, Graph represents the % of $Tbr2^+$ cells colabeled with Olig2 in the VZ/SVZ of DMSO- and FGF15-treated slices ($n = 3$ experiments [2 or 3 slices each experiment] per treatment condition). The percentage of $Tbr2^+$ coexpressing Olig2 is approximately fourfold in FGF15-treated over control DMSO-treated slices and is significantly higher ($^*p \leq 0.05$). Values of statistics are shown in Table 1. Bar graphs represent average values. Error bars indicate SEM.

specification program is maintained by neural progenitors to generate precise numbers and lineages, relying on spatially and temporally modulated molecular cues present in neurogenic niches of the embryonic forebrain. Our study identified SHH and FGF15 signaling as key pathways that must be tightly modulated to ensure successful differentiation of neocortical progenitors into distinct excitatory neuron lineages in the course of corticogenesis (Fig. 8). These findings further underscore the importance of key modulatory factors at crucial time points in establishing and maintaining neocortical progenitor programs.

Neuronal lineage progression relies on the molecular makeup of the neurogenic niche at E12.5

Embryonic neocortical progenitors must follow strict lineage programs throughout corticogenesis to ensure the production of molecularly and functionally diverse excitatory neurons in the mature neocortex. Here, we determined that molecular events in early corticogenesis ensure proper lineage progression of neocortical progenitors. This process relies on tightly inhibiting SHH signaling activity. While pallial-specific progenitors, such as $Pax6^+$ RGCs or $Tbr2^+$ IPCs, are produced in the Sufu-cKO neocortex, these progenitors possessed underlying transcriptomic changes compromising their lineage progression. Many of these changes involved extracellular or plasma membrane-bound proteins, which can substantially alter intercellular and extracellular interactions within the neurogenic niche. Further, we found that subpallial-specific gene transcripts were already ectopically expressed in the E12.5 Sufu-cKO. These indicated that while proteins encoded by these genes may not be detected in neocortical progenitors at E12.5, the stage has been set to alter their fates. Ultimately, these early alterations can permanently deviate lineage programs of neocortical progenitors, resulting in the production of misspecified excitatory neurons in the postnatal neocortex of Sufu-cKO mice.

SHH signaling alters IPC production by preventing lineage progression of RGCs

IPC production is especially vulnerable to varying activity levels of SHH signaling. High SHH signaling activity inhibits IPC production at early stages of corticogenesis but promotes IPC production at later stages (Shikata et al., 2011; H. Wang et al., 2011; Yabut et al., 2015, 2016; L. Wang et al., 2016). While these studies established the mitogenic effect of SHH signaling to control neocortical progenitor proliferation, including IPCs, a growing number of studies are beginning to identify a role for SHH signaling in altering progenitor specification as a parallel means of controlling IPC production. SHH signaling partly mediates this effect via Gli3R activity, which when absent or reduced, can significantly impair specification of neocortical progenitors into distinct excitatory neuron subtypes (H. Wang et al., 2011; Yabut et al., 2015; Hasenpusch-Theil et al., 2018). Supporting these findings, we found upregulated expression of known Gli3R gene targets in the E12.5 Sufu-cKO neocortex, such as *FGF15*, in the progenitor-rich VZ/SVZ where Gli3 is typically highly expressed particularly in RGCs (Rash and Grove, 2007; Pollen et al., 2014; Hasenpusch-Theil et al., 2015; Kim et al., 2018). Specifically, we found an increase in SHH signaling activation (as detected through an increase in *PTCH1* expression) correlating with an increase in *FGF15* expression in RGCs lining the VZ. We found a uniform increase in ectopic *FGF15* expression in the E12.5 Sufu-cKO neocortex. Despite this, RGCs lining the VZ exhibited variable proliferation rates (Yabut et al., 2015), indicating that FGF15 did not have a consistent effect on progenitor proliferation across the neocortical expanse. Rather, we consistently found that the increase in FGF15 levels, in the Sufu-cKO embryonic neocortex or when added in cultured forebrain slices, inhibited the specification of RGCs into bona fide pallial IPCs. Together, our findings expand evidence of the importance of modulating SHH signaling in RGCs, particularly via Gli3 activity, in ensuring lineage progression toward the specification of IPCs into distinct excitatory neuron subtypes.

SHH signaling requires FGF signaling to alter neuronal lineage progression of neocortical progenitors

Our findings revealed that SHH signaling activated FGF signaling leading to disruption of neocortical progenitor specification. Particularly, an increase in FGF15 expression was sufficient to drive these defects. Previous studies showed that FGF15 functions to control progenitor proliferation and differentiation (Borello et al., 2008; Wilson et al., 2012). Supporting a role for FGF15 in proliferation, we found that increased *FGF15* expression correlated with the elongation of the E12.5 Sufu-cKO

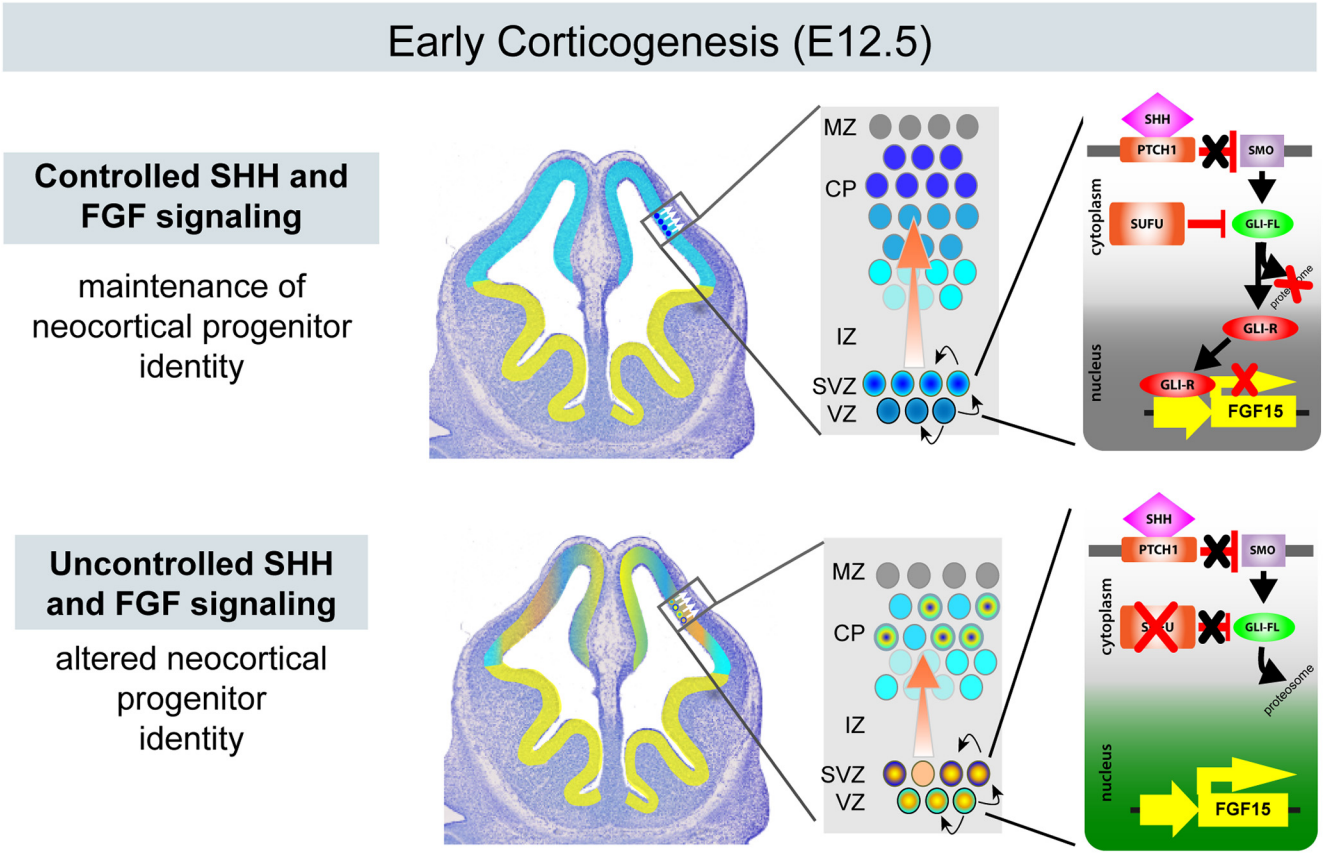

Figure 8. Schematic diagram of how modulation of SHH and FGF signaling affects neocortical progenitors at early stages of corticogenesis. Controlled SHH and FGF signaling, resulting from the repressive function of Gli3R, in the dorsal forebrain, maintains the neocortical identity and specification program of progenitors. Uncontrolled SHH and FGF signaling, achieved when Sufu expression is lost consequently leading to Gli3 degradation and the eventual upregulation of FGF15 expression, results in the inability of neocortical progenitors to maintain the dorsal forebrain identity and specification program.

neocortex. However, as mentioned, FGF15 upregulation did not uniformly correlate with proliferation defects. Supporting this, we found variable levels of activation in MAPK signaling, the downstream intracellular FGF signaling effector. MAPK signaling activity was distinctly higher in dorsal and dorsolateral regions of the E12.5 Sufu-cKO neocortex, but not in dorsomedial regions where FGF15 was also ectopically expressed. Additionally, clonally related progenitors in the rostral neocortical regions of the E12.5 Sufu-cKO neocortex appeared to be uniquely affected. Columnar patterns in the expression levels of Pax6, Olig2, and MAPK activity levels are apparent. These observations suggest that FGF15 differentially affects molecularly distinct neocortical progenitors, which may be predicted by their spatial and temporal localization in the embryonic neocortex. These varying effects may result in changes to cell cycle length, neuronal differentiation, or their specification programs.

While it may be logical to assume that FGF15 will predictably bind to progenitors expressing its cognate receptor, FGFR4, FGFR4 has not been detected in the E12.5 neocortex (Harmer et al., 2004; Tole et al., 2006; Zhang et al., 2006; Borello et al., 2008). On the other hand, FGFR1-3 are expressed in varying levels and spatial domains across the E12.5 neocortical wall and may be sensitive to high levels of FGF15 (Tole et al., 2006; Borello et al., 2008). Alternatively, global changes in the molecular make-up of the E12.5 Sufu-cKO neurogenic niche may have facilitated unique FGF15 interactions. This may explain why Sufu-cKO mice do not completely phenocopy mouse mutants carrying conditional Gli3R mutations (H. Wang et al., 2011; Hasenpusch-Theil et al., 2018). Together, these findings underscore the complexity of FGF15 function in the developing neocortex. Future studies require further elucidation of the molecular properties of FGF15-responsive neocortical progenitors and the signaling pathways transduced to elicit changes in progenitor behavior.

In conclusion, along with the expansion and diversification of neocortical neuron subtypes in the developing brain, anomalies in the production of diverse excitatory neurons underlie a number of neuropsychiatric and neurodevelopmental disorders. The activation of FGF and MAPK signaling cascades, in response to SHH signaling activation, indicates important potential implications of uncontrolled SHH signaling in these disorders. For instance, it is evident that abnormal numbers and specification of neuronal subtypes lead to aberrant circuits in autism spectrum disorders (Kaushik and Zarbalis, 2016). High serum levels of SHH and deregulated FGF signaling activity at developmental stages has been implicated in these defects (Vaccarino et al., 2009; Rubenstein, 2011; Al-Ayadhi, 2012; Halepoto et al., 2015). Activation of SHH signaling at early stages of corticogenesis, consequently driving FGF signaling, may profoundly alter the molecular landscape of neocortical progenitors and their progenies. Thus, further investigation of how pathogenic SHH and FGF signaling converge to produce aberrant neuronal subtypes and neocortical circuitry could lay the

foundation toward detecting, treating, or even reversing the neocortical abnormalities present in neurodevelopmental disorders.

References

Al-Ayadhi LY (2012) Relationship between sonic hedgehog protein, brain-derived neurotrophic factor and oxidative stress in autism spectrum disorders. Neurochem Res 37:394–400.

Beattie R, Hippenmeyer S (2017) Mechanisms of radial glia progenitor cell lineage progression. FEBS Lett 591:3993–4008.

Borello U, Cobos I, Long JE, McWhirter JR, Murre C, Rubenstein JL (2008) FGF15 promotes neurogenesis and opposes FGF8 function during neocortical development. Neural Dev 3:17.

Dave RK, Ellis T, Toumpas MC, Robson JP, Julian E, Adolphe C, Bartlett PF, Cooper HM, Reynolds BA, Wainwright BJ (2011) Sonic hedgehog and notch signaling can cooperate to regulate neurogenic divisions of neocortical progenitors. PLoS One 6:e14680.

Fotaki V, Yu T, Zaki PA, Mason JO, Price DJ (2006) Abnormal positioning of diencephalic cell types in neocortical tissue in the dorsal telencephalon of mice lacking functional Gli3. J Neurosci 26:9282–9292.

Gimeno L, Martinez S (2007) Expression of chickFgf19 and mouseFgf15 orthologs is regulated in the developing brain byFgf8 andShh. Dev Dyn 236:2285–2297.

Guillemot F, Zimmer C (2011) From cradle to grave: the multiple roles of fibroblast growth factors in neural development. Neuron 71:574–588.

Halepoto DM, Bashir S, Zeina R, Al-Ayadhi LY (2015) Correlation between hedgehog (Hh) protein family and brain-derived neurotrophic factor (BDNF) in autism spectrum disorder (ASD). J Coll Physicians Surg Pak 25:882–885.

Harmer NJ, Pellegrini L, Chirgadze D, Fernandez-Recio J, Blundell TL (2004) The crystal structure of fibroblast growth factor (FGF) 19 reveals novel features of the FGF family and offers a structural basis for its unusual receptor affinity. Biochemistry 43:629–640.

Hasenpusch-Theil K, Watson JA, Theil T (2015) Direct interactions between Gli3, Wnt8b, and Fgfs underlie patterning of the dorsal telencephalon. Cereb Cortex 27:1137–1148.

Hasenpusch-Theil K, West S, Kelman A, Kozic Z, Horrocks S, McMahon AP, Price DJ, Mason JO, Theil T (2018) Gli3 controls the onset of cortical neurogenesis by regulating the radial glial cell cycle through Cdk6 expression. Development 145:dev163147.

Hevner RF (2019) Intermediate progenitors and Tbr2 in cortical development. J Anat 235:616–625.

Huang DW, Sherman BT, Tan Q, Collins JR, Alvord WG, Roayaei J, Stephens R, Baseler MW, Lane HC, Lempicki RA (2007) The DAVID Gene Functional Classification Tool: a novel biological module-centric algorithm to functionally analyze large gene lists. Genome Biol 8:R183.

Huang da W, Sherman BT, Lempicki RA (2009) Systematic and integrative analysis of large gene lists using DAVID bioinformatics resources. Nat Protoc 4:44–57.

Kaushik G, Zarbalis KS (2016) Prenatal neurogenesis in autism spectrum disorders. Front Chem 4:12.

Kim JJ, Jiwani T, Erwood S, Loree J, Rosenblum ND (2018) Suppressor of fused controls cerebellar neuronal differentiation in a manner modulated by GLI3 repressor and Fgf15. Dev Dyn 247:156–169.

Komada M, Saitsu H, Kinboshi M, Miura T, Shiota K, Ishibashi M (2008a) Hedgehog signaling is involved in development of the neocortex. Development 135:2717–2727.

Komada M, Saitsu H, Shiota K, Ishibashi M (2008b) Expression of Fgf15 is regulated by both activator and repressor forms of Gli2 in vitro. Biochem Biophys Res Commun 369:350–356.

Long F, Zhang XM, Karp S, Yang Y, McMahon AP (2001) Genetic manipulation of hedgehog signaling in the endochondral skeleton reveals a direct role in the regulation of chondrocyte proliferation. Development 128:5099–5108.

Miyoshi G, Butt SJ, Takebayashi H, Fishell G (2007) Physiologically distinct temporal cohorts of cortical interneurons arise from telencephalic Olig2-expressing precursors. J Neurosci 27:7786–7798.

Palma V, Ruiz i Altaba A (2004) Hedgehog-GLI signaling regulates the behavior of cells with stem cell properties in the developing neocortex. Development 131:337–345.

Petryniak MA, Potter GB, Rowitch DH, Rubenstein JL (2007) Dlx1 and Dlx2 control neuronal versus oligodendroglial cell fate acquisition in the developing forebrain. Neuron 55:417–433.

Pollen AA, Nowakowski TJ, Shuga J, Wang X, Leyrat AA, Lui JH, Li N, Szpankowski L, Fowler B, Chen P, Ramalingam N, Sun G, Thu M, Norris M, Lebofsky R, Toppani D, Kemp DW, Wong M, Clerkson B, Jones BN, et al. (2014) Low-coverage single-cell mRNA sequencing reveals cellular heterogeneity and activated signaling pathways in developing cerebral cortex. Nat Biotechnol 32:1053–1058.

Pospisilik JA, Schramek D, Schnidar H, Cronin SJF, Nehme NT, Zhang X, Knauf C, Cani PD, Aumayr K, Todoric J, Bayer M, Haschemi A, Puviindran V, Tar K, Orthofer M, Neely GG, Dietzl G, Manoukian A, Funovics M, Prager G, et al. (2010) Drosophila genome-wide obesity screen reveals hedgehog as a determinant of brown versus white adipose cell fate. Cell 140:148–160.

Rash BG, Grove EA (2007) Patterning the dorsal telencephalon: a role for sonic hedgehog? J Neurosci 27:11595–11603.

Rubenstein JL (2011) Annual Research Review: development of the cerebral cortex: implications for neurodevelopmental disorders. J Child Psychol Psychiatry 52:339–355.

Shikata Y, Okada T, Hashimoto M, Ellis T, Matsumaru D, Shiroishi T, Ogawa M, Wainwright B, Motoyama J (2011) Ptch1-mediated dosage-dependent action of Shh signaling regulates neural progenitor development at late gestational stages. Dev Biol 349:147–159.

Siegenthaler JA, Ashique AM, Zarbalis K, Patterson KP, Hecht JH, Kane MA, Folias AE, Choe Y, May SR, Kume T, Napoli JL, Peterson AS, Pleasure SJ (2009) Retinoic acid from the meninges regulates cortical neuron generation. Cell 139:597–609.

Sohal VS, Rubenstein JL (2019) Excitation-inhibition balance as a framework for investigating mechanisms in neuropsychiatric disorders. Mol Psychiatry 24:1248–1257.

Tole S, Gutin G, Bhatnagar L, Remedios R, Hébert JM (2006) Development of midline cell types and commissural axon tracts requires Fgfr1 in the cerebrum. Dev Biol 289:141–151.

Toresson H, Potter SS, Campbell K (2000) Genetic control of dorsal-ventral identity in the telencephalon: opposing roles for Pax6 and Gsh2. Development 127:4361–4371.

Vaccarino FM, Grigorenko EL, Smith KM, Stevens HE (2009) Regulation of cerebral cortical size and neuron number by fibroblast growth factors: implications for autism. J Autism Dev Disord 39:511–520.

Wang H, Ge G, Uchida Y, Luu B, Ahn S (2011) Gli3 is required for maintenance and fate specification of cortical progenitors. J Neurosci 31:6440–6448.

Wang L, Hou S, Han YG (2016) Hedgehog signaling promotes basal progenitor expansion and the growth and folding of the neocortex. Nat Neurosci 19:888–896.

Wang Y, Kim E, Wang X, Novitch BG, Yoshikawa K, Chang LS, Zhu Y (2012) ERK inhibition rescues defects in fate specification of Nf1-deficient neural progenitors and brain abnormalities. Cell 150:816–830.

Wilson SL, Wilson JP, Wang C, Wang B, McConnell SK (2012) Primary cilia and Gli3 activity regulate cerebral cortical size. Dev Neurobiol 72:1196–1212.

Yabut OR, Fernandez G, Huynh T, Yoon K, Pleasure SJ (2015) Suppressor of fused is critical for maintenance of neuronal progenitor identity during corticogenesis. Cell Rep 12:2021–2034.

Yabut OR, Ng H, Fernandez G, Yoon K, Kuhn J, Pleasure SJ (2016) Loss of suppressor of fused in mid-corticogenesis leads to the expansion of intermediate progenitors. J Dev Biol 4:29.

Ypsilanti AR, Rubenstein JL (2016) Transcriptional and epigenetic mechanisms of early cortical development: an examination of how Pax6 coordinates cortical development. J Comp Neurol 524:609–629.

Zhang X, Ibrahimi OA, Olsen SK, Umemori H, Mohammadi M, Ornitz DM (2006) Receptor specificity of the fibroblast growth factor family: the complete mammalian FGF family. J Biol Chem 281:15694–15700.